WWF
REPORT
PAK
2012

ccap

Delta Wide Hazard Mapping
- A Case Study of Keti Bunder, Kharo Chann and Jiwani

December 2012

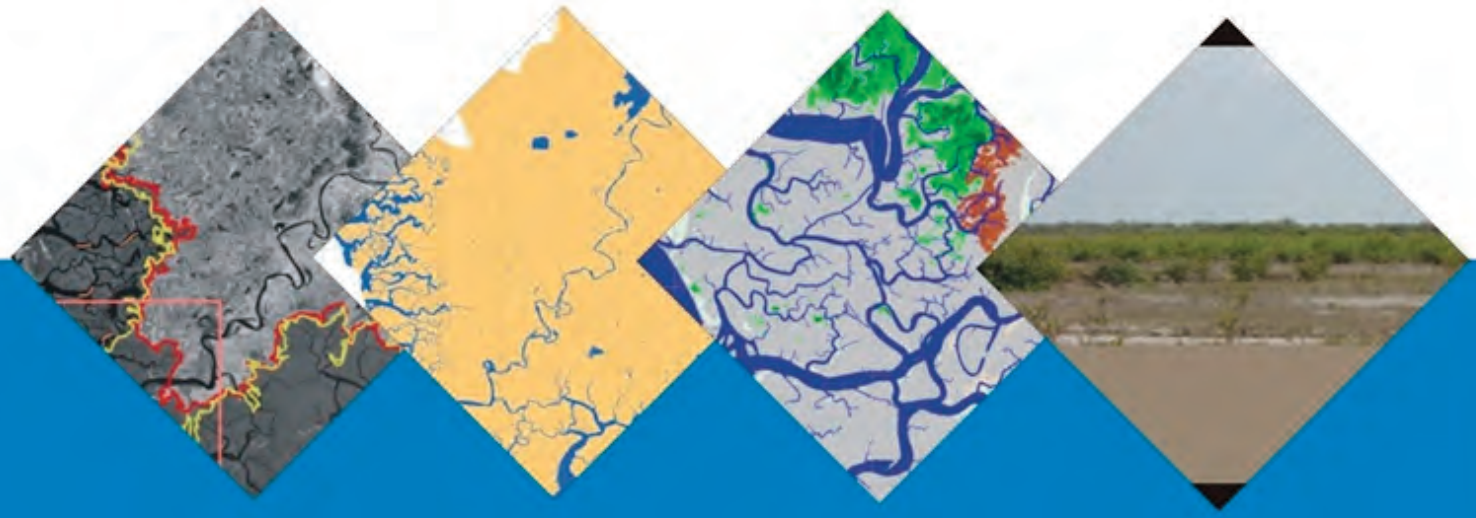

GIS Laboratory, WWF - Pakistan

Delta Wide Hazard Mapping – A Case Study of Keti Bunder, Kharo Chann and Jiwani

Draft Report

Submitted on 07th Decemberr 2012

GIS Laboratory, WWF - Pakistan

Members contributed: (in alphabetical order)

ArsheenNasir
Hassan Ali
Irfan Ashraf
NaeemShahzad
Syed GhulamMohayud Din Hashmi
Syed Muhammad Irteza
WasifYousaf
UroojSaeed
ZainulAbidin

Title: Delta Wide Hazard Mapping Study – A Case Study(Keti Bunder, Kharo Chann and Jiwani)

Correspondence: gislab@wwf.org.pk

© The GIS Laboratory, World Wide Fund for Nature (WWF) – Pakistan

This publication may be of assistance to readers, however, the GIS Lab, WWF-Pakistan and its employees do not guarantee that the publication is without flaw of any kind or is wholly appropriate for their particular purposes, therefore disclaims all liability for any error, loss or other consequences which may arise from your relying on information in this publication.

Photo credits: GIS Laboratory, WWF – Pakistan

Abbreviations

AOI	Area of Interest
ASTER	Advanced Space-borne Thermal Emission and Reflection Radiometer
DEM	Digital Elevation Model
E	East
FAO	Food and Agriculture Organization of the United Nations
FCCs	False Color Composites
GDEM	Global Digital Elevation Model
GOP	Government of Pakistan
GPS	Global Positioning System
km	kilometer
LC/LU	Land Cover Land Use
m	meter
N	North
OBIA	Object Based Image Analysis
SoP	Survey of Pakistan
WWW	World Wide Web
yr	year

Contents

ABBREVIATIONS III

LIST OF FIGURES VI

LIST OF TABLES VII

1 INTRODUCTION 1

2 PROJECT AREA 1

3 OBJECTIVES OF THE STUDY 1

4 BASE MAP DEVELOPMENT AND LAND COVER CLASSIFICATION 2

4.1 TOPO CADASTRAL MAPPING 2

4.2 SATELLITE IMAGE CLASSIFICATION AND CHANGE DETECTION 2

4.2.1 Acquisition of Satellite Data 2

4.2.2 Pre-processing 3

4.2.3 Ground Truthing 4

4.2.4 Satellite Image Segmentation 5

4.2.5 Rule Set Development 5

4.2.6 Work Flow Diagram for Classification 5

4.2.7 Software Used 6

5 LAND COVER/LAND USE CHANGE ANALYSIS 7

5.1 CHANGE ANALYSIS OF KETI BUNDER 7

5.1.1 Land cover derived from 2001 satellite data 7

5.1.2 Land cover derived from 2011 satellite data 7

5.2 CHANGE ANALYSIS OF KHARO CHANN 10

5.2.1 Land cover derived from 2001 satellite data 10

5.2.2 Land cover derived from 2011 satellite data 10

5.3 CHANGE ANALYSIS OF JIWANI 13

5.3.1 Land cover derived from 2000 satellite data 13

5.3.2 Land cover derived from 2011 satellite data 13

5.4 CHANGE SLICES IN THE FORESTED AREAS OF PROJECT AREAS 18

6 HAZARD MAPPING 20

6.1 IDENTIFICATION OF HAZARDS IN STUDY AREA 20

6.2 CYCLONE 20
6.3 FLOODS IN PAKISTAN 23
6.3.1 Flood Susceptibility Mapping using Logistic Regression 25
6.4 LAND EROSION/ACCRETION 34
6.5 METEOROLOGICAL PARAMETERS 38
6.6 REFERENCES 42

List of Figures

Figure 1: Study area location map....1

Figure 2: Topo-cadastral Maps 2

Figure 3: Truncation....3

Figure 4: Field observation points of Keti Bunder and Kharo Chann Project sites 4

Figure 5: Field observation points of Jiwani Project Site....5

Figure 6: Segmented layer of the satellite image....5

Figure 7: Flow diagram of Land Cover / Land Use classification 6

Figure 8: LCLU map of Keti Bunder developed for 2001 8

Figure 9: LCLU map of Keti Bunder developed for 2011 9

Figure 10: Graphical representation of historic and current statistics – Keti Bunder 10

Figure 11: LCLU map of Kharo Chann developed for 2001....11

Figure 12: LCLU map of Kharo Chann developed for 2011....12

Figure 13: Graphical representation of historic and current statistics – Kharo Chann....13

Figure 14: LCLU map of Jiwani developed for year 2000....14

Figure 15: LCLU map of Jiwani developed for year 2011....15

Figure 16: Graphical representation of historic and current statistics – Jiwani....16

Figure 17: Increase near Turshan and Tango Creek – Keti Bunder....18

Figure 18: Increase in mangroves cover near Adhiari and Sohnri creek – Kharo Chann....18

Figure 19: Google earth image slice of plantation site (a) 2006 (b) 2012....19

Figure 20: Ground picture taken through Fixed Point Photography of mangroves plantation site in Keti Bunder – left (May 2010) and right (May 2012) 19

Figure 21: (Left) Phet track depicting its movement and intensity, year 2010 (source: TCWC-PMD) (Right) shows the model-simulated surge contours with a maximum value being 1.17 m 21

Figure 22: Intensity map of Cyclone/Tsunami of Gawadar District, Pakistan (1945-2010)....23

Figure 23: Ten biggest natural disasters in Pakistan (Source: UNOCHA) 23

Figure 24: MODIS images - flood extent along the Indus River, Sindh....24

Figure 25: Erosion due to flood 2010 along Indus river in Atharki Village 24

Figure 26: Map showing the AOI used for the study 25

Figure 27: Map showing the land cover of the study area 27

Figure 28: Water Extent in Normal Circumstances 28

Figure 29: Precipitation layers for the minimum and maximum values for past 30 years 29

Figure 30: ASTER GDEM of 30m resolution for the study area 29

Figure 31: Slope and curvature maps derived from ASTER DEM 30

Figure 32: Flow diagram of the flood modeling 31

Figure 33: Direct output for flood susceptible area without precipitation 31

Figure 34: Flood susceptible areas direct output for minimum precipitation (Left) and for maximum precipitation (Right) 32

Figure 35: Flood susceptibility for different precipitation scenarios 32

Figure 36: Map showing flood prediction estimated at three levels for Thatta district 33

Figure 37: Erosion / Accretion change flow chart 34

Figure 38: Near Waddi Khuddi Creek, red line shows the position of coastline in 1962 and the current position in 2011 is in green colour. Trend line highlights erosion of the land in meters. 35

Figure 39: Density Map - Erosion and Accretion Pressure (Keti Bunder and Kharo Chann) 36

Figure 40: Overall soil erosion pressure areas in indus delta 36

Figure 41: Inland deltaic extent of Indus delta 37

Figure 42: A remarkable erosion and accretion, observed along the coastline of Jiwani – Balochistan which basically appears due to the change in overall drainage pattern 38

Figure 43: Precipitation Data taken from FY- Meteorological satellite of the Study area in Indus Delta (1961-1990) 38

Figure 44: Temperature Data taken from FY- Meteorological satellite of the Study area in Indus Delta (1961-1990) 39

Figure 45: Baseline and predicted values of Temperature and precipitation for Thatta District. 41

List of Tables

Table 1: Characteristic details of satellite images 3

Table 2: Statistical details and percentage change of each class in each project site 17

Table 3: Historic data (1964-2010) of TC near the coast of Pakistan 20

Table 4: Major Cyclones/Tsunami and their impact 21

Table 5: Predictor variables used for the intensive and extensive analysis.....26

1 Introduction

Remote Sensing and Geographic Information System (GIS) has emerged as a significant tool to complement conventional methods involved in natural hazard mapping and mitigation. Natural disasters have drastically increased in magnitude and frequency over the last few decades; on the other hand there has been a substantial improvement in technical capabilities to mitigate them. The use of remote sensing data, such as satellite images, aerial photographs along with various geospatial analyses provides a significant source to map and identify the disaster prone areas. Satellite images give a synoptic overview and provide useful information, for a wide range of scales, from entire continents to detail of a few meters. Disasters, such as floods, droughts and cyclones have certain precursors that satellite can detect. Remote sensing also allows mapping and monitoring of the event as it occurs.

This study discusses the land cover / land use changes (forest change, land erosion and accretion and the impact and intensity of various natural hazards) through using satellite images and geospatial technology.

2 Project Area

This study focuses on the selected areas of the Pakistan coast covering part of Indus Delta and Balochistan coast. Keti Bunder and Kharo Channhas been prioritized from Indus Delta of Sindh Province and Jiwanifrom Gwadar District,BalochistanProvince(Figure 1).

Figure 1:Study area location map

3 Objectives of the Study

The objectives of this study are to;

- Establish GIS - based spatial data layers using Survey of Pakistan (SoP) topographic sheets
- Conduct land cover/land use change analysis of the selected sites using multi temporal satellite images
- Estimate land erosion along the Indus Delta and Jiwani coast
- Flood impact assessment and identification of flood prone areas using historic datasets
- Develop hazard maps and perform different spatial analysis to identify the secure areas for the local community.

4 Base Map Development and Land Cover Classification

4.1 Topo Cadastral Mapping

To generate geographic layers of different topographic features such as administrative boundaries, infrastructures andtoponyms (habitation, landmarks, hydrology etc), geo-scanned Survey of Pakistan (SoP) topographic maps were used. Topographic layers of Indus Delta were extracted from 1: 250,000 whereas 1:50,000 sheets were used for the selected project sites (Figure 2).

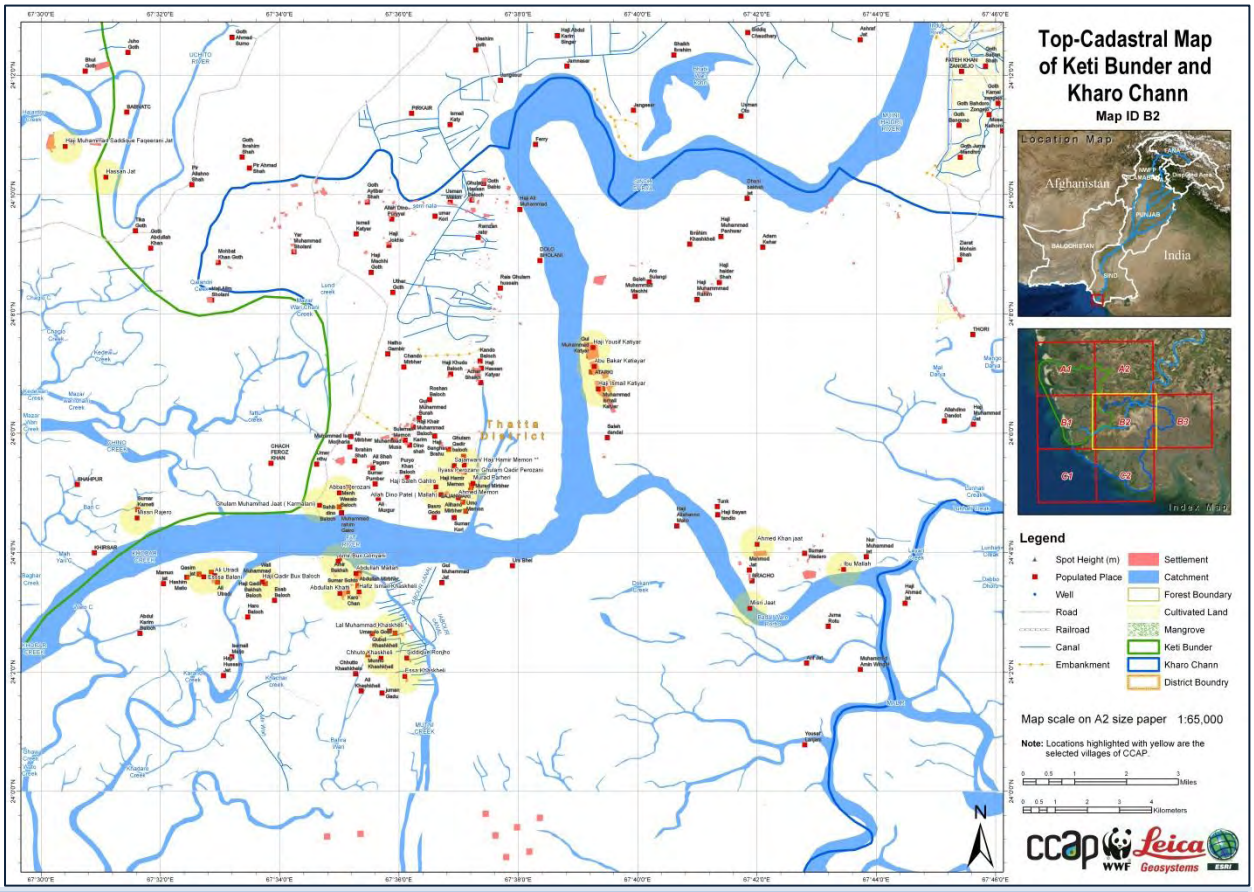

Figure 2: Topo-cadastral Maps

4.2 Satellite Image Classification and Change Detection

Classification is the process of assigning pixels of a continuous raster image to predefined classes.In this study the advanced and most recent classification technique i.e. Object Based Image Analysis (OBIA) was applied on the satellite images. Following fundamental steps were adopted for the mapping using Object Based Classification in Definien Developer®.

4.2.1 Acquisition of Satellite Data

Historic and current satellite images of Terra (ASTER) were procured from the Earth Remote Sensing Data Analysis (ERSDA) centre, Japan. During procurement, parameters that control image quality such as tide heights, nadir angle, atmosphericclarity and cloud free data sets have been preferred. The characteristics of the procured images are shown in the following table 1.

Table 1: Characteristic details of satellite images

Project Site	Acquisition Date	Spatial Resolution - VNIR (m)	Spectral Bands	Tide Height (m)
Kharo Chann	December 24, 2001	15	14	1.2
	January 2, 2011	15	14	1.2
Keti Bunder	December 24, 2001	15	14	2.6
	January2, 2011	15	14	2.6
Jiwani	October 30, 2000	15	14	2.3
	June 5, 2011	15	14	2.3

Keyhole/Corona (1962) from 'American Imaging' has been procured in order to estimate the change in the extent of the coastal line. The historic (Keyhole/Corona) datasets are available only insingle layer of grey levels and are not suitable for image classification i.e. forest cover extraction to some extent. However, the significance of the historic datasets can never be neglected when it comes to the comparison and identification of the historical picture on the basis of visual interpretation and manual data extraction of the sea line and other land features.

4.2.2 Pre-processing

Import

The images were acquired in *Hierarchical Data* (*.hdf*) *format*. For easy handling and processing, images were imported in ERDAS Imagine native image format (*.img*) by importing all the available bands with the file.

Truncation of Study Area

In order to save the lavish time which takes a long processing time and computer resources, it has been recommended to subset the satellite image at a desired Areas of Interest (AOI) i.e. project sites. Satellite images were truncated at the boundary of Kharo ChannTaluka, Keti Bunder Indus for All programme project site and Jiwani. The truncation also provideda high level of confidence at training sites selection, hence enhanced the overall accuracy of the results (Figure 3).

Figure 3: Truncation

Satellite Image Enhancement

Due to inherent low contrast, satellite data always require enhancement of specific feature of interest using various image enhancement algorithms. Keeping in view the subjective land cover, Histogram Equalize and Standard Deviation Stretch were applied for the extraction of meaningful information regarding different land cover classes. These algorithms enhanced the low contrast of satellite images and made them more interpretable for further processing. Moreover, the brightness and contrast utility as well as different False Colour Composites (FCCs) were used to enhance the image interpretability.

4.2.3 Ground Truthing

Ground truthing is the acquisition of knowledge about the study area from field. It also refers to the acquisition of knowledge about the study area from the analysis of aerial photography, personal experience etc.The main objective of ground truthingis to correlate the reflectance values of the satellite image with the ground realities by collecting the Global Positioning System (GPS) coordinates of the training samples for land cover mapping. For ground truth data collection, a field visit was conducted from 22nd to 26th May, 2012 for Keti Bunder and Kharo Chann project sites.

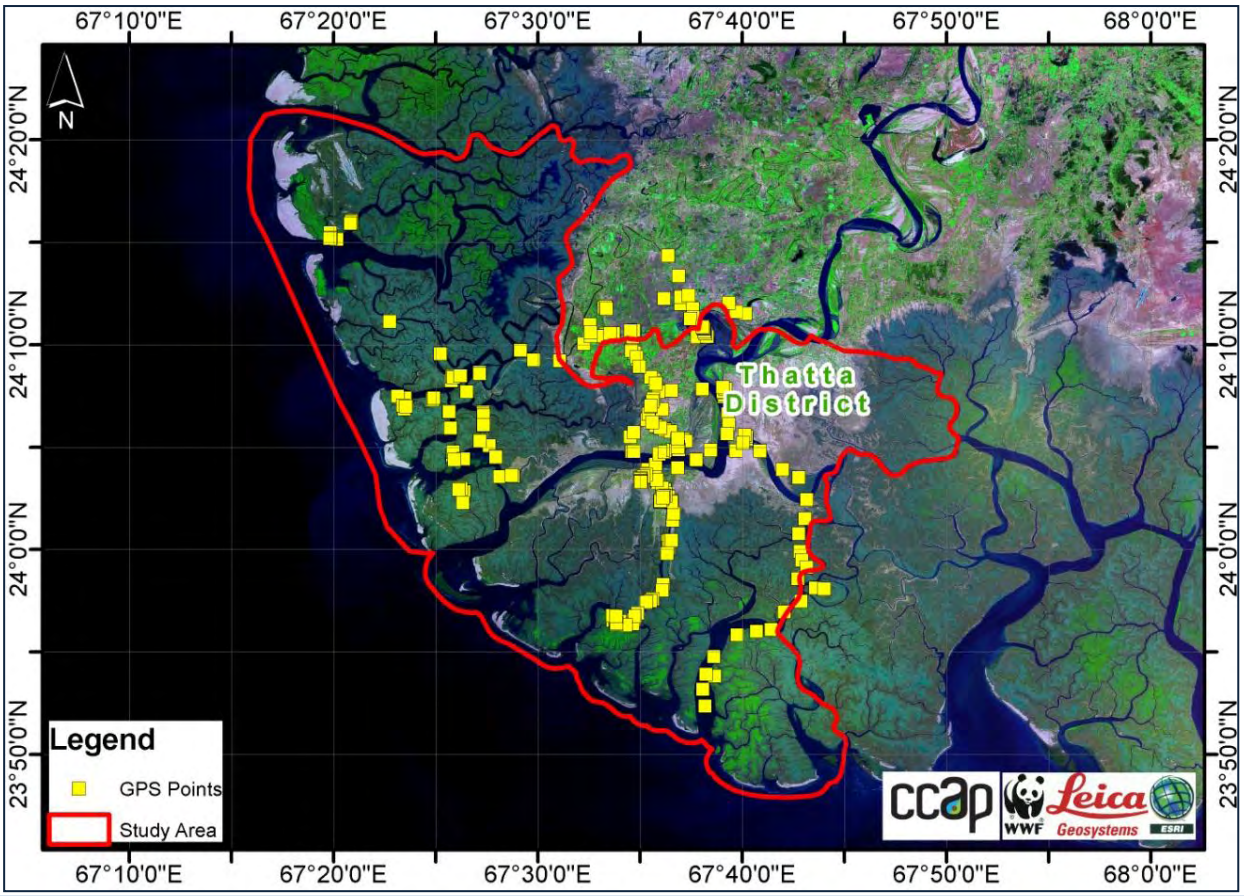

Figure 4: Field observation points of Keti Bunder and Kharo Chann Project sites

Garmin 76CSX Global Positioning System (GPS) receiverand a digital camera were used to collect eighty-oneGPS points (Figure 4). Land vehicle and boat were used to navigate in the field. Land vehicles were used to take observations of the inland areas by road. Whereas, the observations of mangroves along narrow creeks and around the peripheries of mud flats were made possible by the boat.In Jewini, the survey team was not able to conduct the field activities and hence the ground truth data already available in the archieve was used for the analysis as shown in Figure 5.

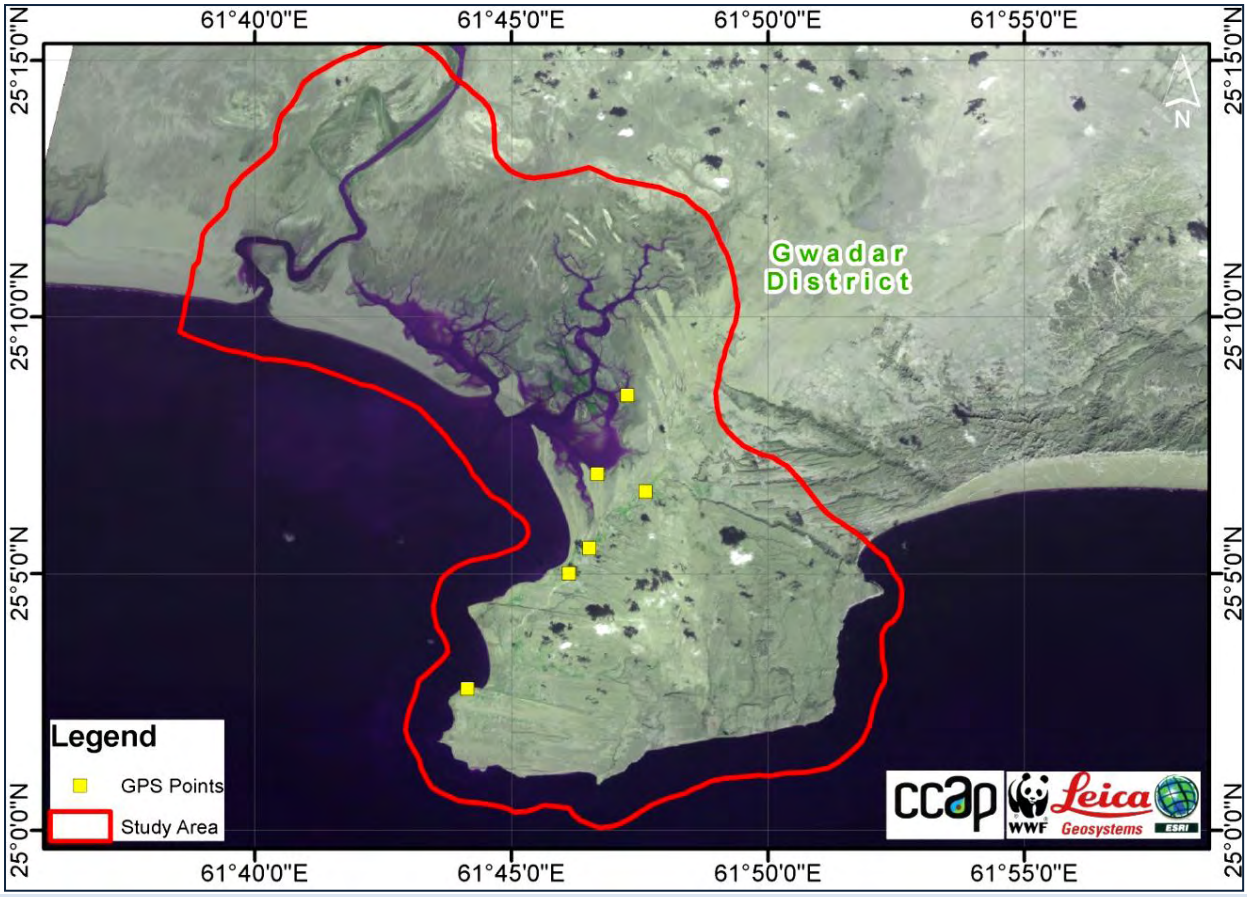

Figure 5: Field observation points of Jiwani Project Site

4.2.4 Satellite Image Segmentation

Segmentation is a process of defining discrete objects or classes of object on the satellite image.

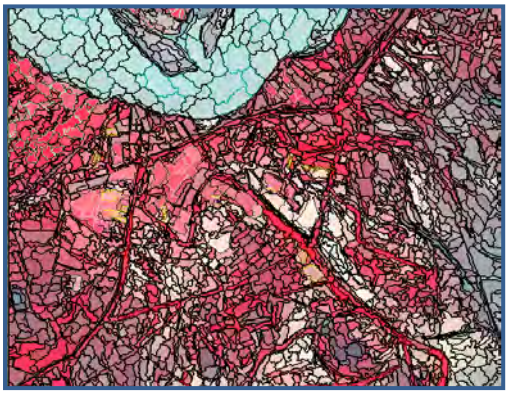

Figure 6: Segmented layer of the satellite image

4.2.5 Rule Set Development

A rule set is basically set of algorithms that defines or runs in process tree to assign classes to image object domain on the basis of defined algorithm. Moreover, the rule set is the sequence of the processes that are executed in the defined order to classify the classes. For the land cover change analysis, different parameters were used to define the rule set for the extraction of the existing features/classes.

4.2.6 Work Flow Diagram for Classification

Temporal thematic maps were generated on historic and current data sets of all the project sites. The flow chart describes the method adopted for the change analysis.

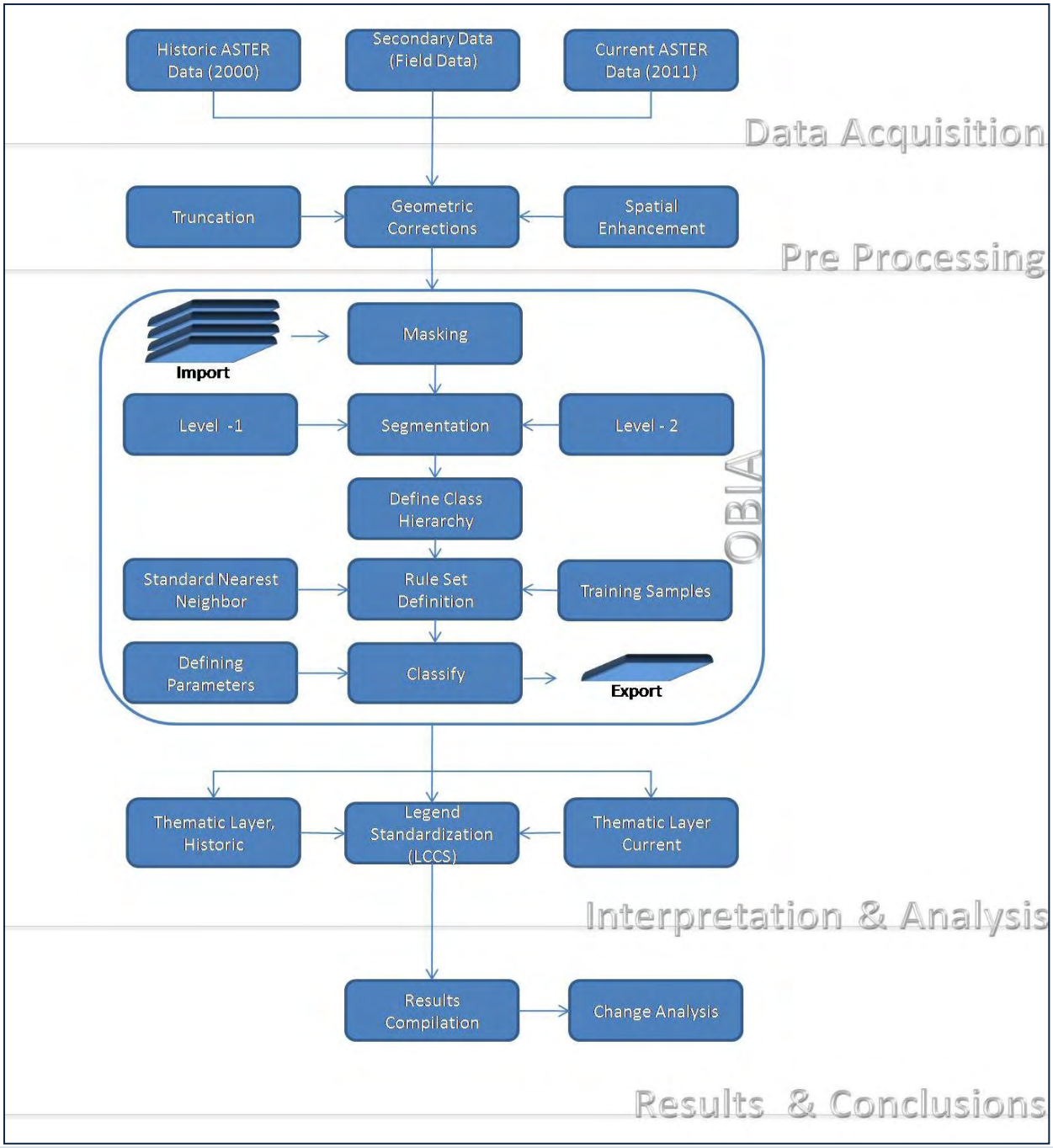

Figure 7: Flow diagram of Land Cover / Land Use classification

4.2.7 Software Used

For interpretation and processing, Digital Image Processing (DIP) software ERDAS Imagine 8.7® and Definien Developer 7.0® were used. Land Cover Classification System (LCCS) sofware, developed by Food and Agricultute Organization (FAO) has been used for land cover stabderdzation. All the maps were developed in ArcGIS 9.3®. Microsoft Word and Microsoft Excel were used for documentation and graphical analysis. Field maps, Garmin GPS 76 CSX receiver and Canon PowerShot SX1 IS digital camera were used for field navigation and data recording.

5 Land Cover/Land Use Change Analysis

5.1 Change Analysis of Keti Bunder

5.1.1 Land cover derived from 2001 satellite data

Based on Aster image of 2001, the mangrove canopy cover analysis show that the total mangroves cover in the area was about 7,536 ha. Closed canopy mangroves cover was about 1,529 ha (20%), closed to open canopy mangrove cover was about 1,282 ha (17%), open mangrove cover was about 2,880 ha (38%) and open canopy (10-30 %) mangrove cover was about 1,985 ha (26%). Mix class of Saltbush/grasses covers an area about 574 ha.

In addition, some of the pure patches of algae were also identified and delineated along the inland side which cover an area of 1,158 ha approx.

5.1.2 Land cover derived from 2011 satellite data

From the analysis of Aster image of 2011, it was noted that the total mangrove cover in Keti Bunder is 7,774 ha, out of which closed canopy mangrove cover is about 1,628 ha (21%), closed to open canopy mangrove cover is about 1,467 ha (19%), open canopy mangrove cover is about 2,988 ha (38%) and open canopy (10-30%) mangrove cover is about 1,689 ha (22%). In addition thin/sparse algal mats spread over 159 ha of land were delineated from 2011s dataset.

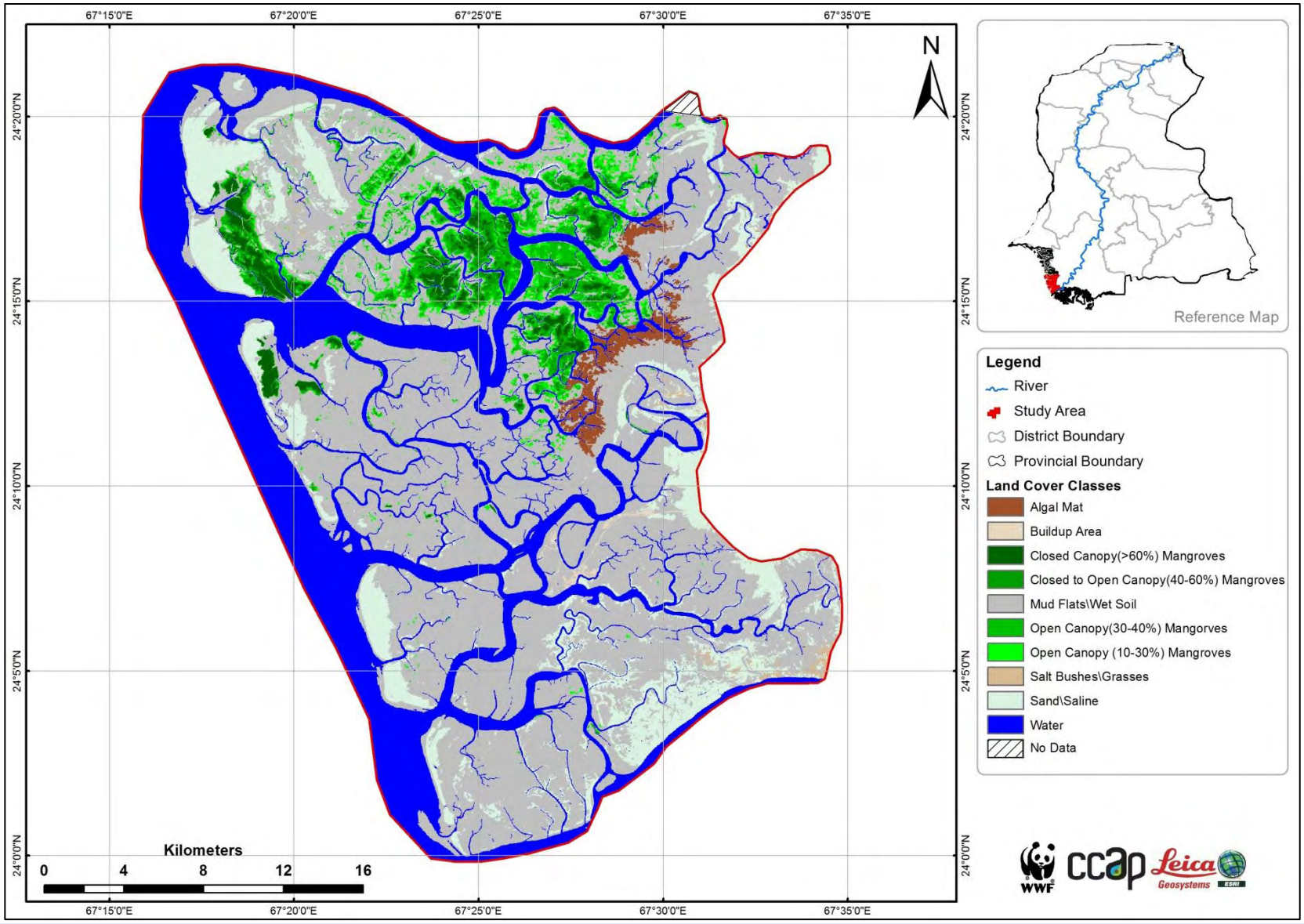

Figure 8: LCLU map of Keti Bunder developed for 2001

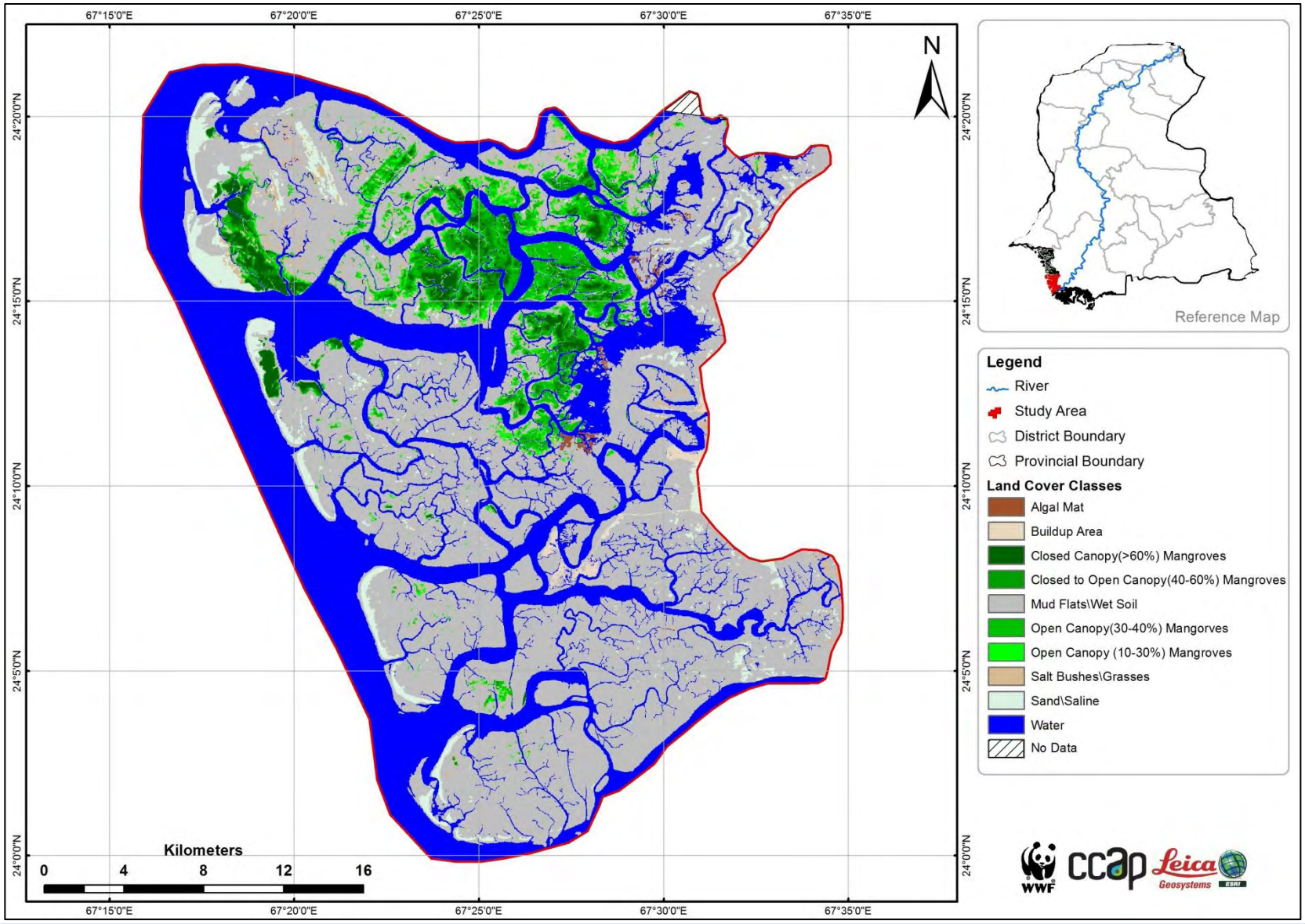

Figure 9: LCLU map of Keti Bunder developed for 2011

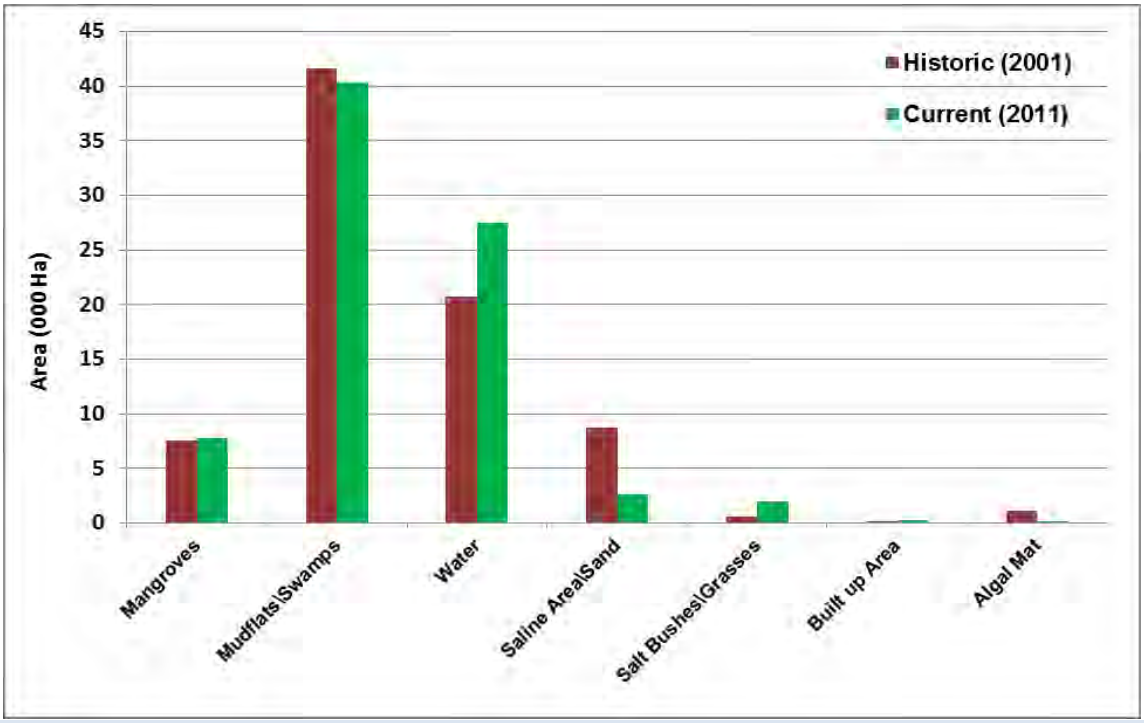

Figure 10: Graphical representation of historic and current statistics – Keti Bunder

5.2 Change Analysis of Kharo Chann

The output land cover maps contains three categories of the vegetation types of in Kharo Chann i.e.

1 Deltaic vegetation comprises of mangroves and saltbushes
2 Riparian vegetation is along the Indus River and its outshoots. It mainly contains *Tamarix* spp., *Mesquite* spp., Reeds and at a few places some trees of *Acacia* spp.
3 Terrestrial vegetation comprises of the roadside plantations, natural trees along the agriculture fields/tracks and other inland scattered vegetation.

5.2.1 Land cover derived from 2001 satellite data

Based on Aster image of 2001, the mangrove canopy cover analysis shows that the total mangrove cover in Kharo Chann was about 5,184 ha. Closed canopy mangrove cover was about 1,523 ha (29%), closed to open canopy mangrove cover was about 773 ha (15%), open mangrove cover was about 1,729 ha (33%) and open canopy (10-30 %) mangrove cover was about 1,158 ha (22%). Mix class of Saltbush/grasses class covers an area about 3,165 ha.

In addition closed canopy *Mesquite*spp/*Tamarix*spp/ Bushes cover wasabout 744 ha and open canopy *Mesquite*spp/*Tamarix*spp/ Bushes cover was about 1,793 ha.

5.2.2 Land cover derived from 2011 satellite data

From the analysis of Aster image of 2011, it was noted that the total mangrove cover in Kharo Chann is 7,752 ha, out of which closed canopy mangrove cover is about 1,956 ha (25%), closed to open canopy mangrove cover is about 1,197 ha (15%), open canopy mangrove cover is about 2,710 ha (35%) and open canopy (10-30%) mangrove cover is about 1,887 ha (24%). In addition closed canopy *Mesquite*spp/*Tamarix*spp/ Bushes spread over 673 ha and open canopy *Mesquite*spp/*Tamarix*spp/ Bushes cover is about 1,491 ha.

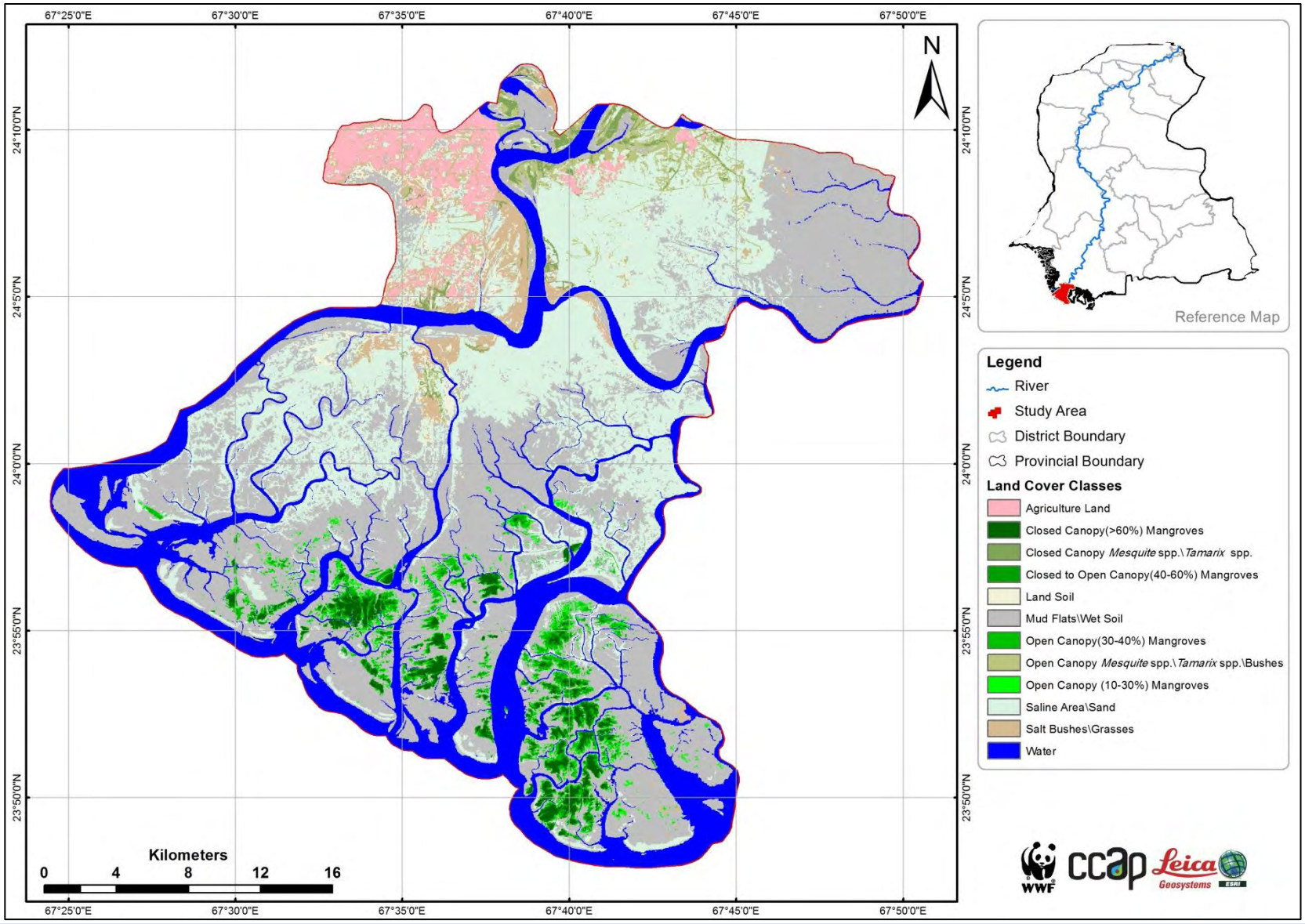

Figure 11: LCLU map of Kharo Chann developed for 2001

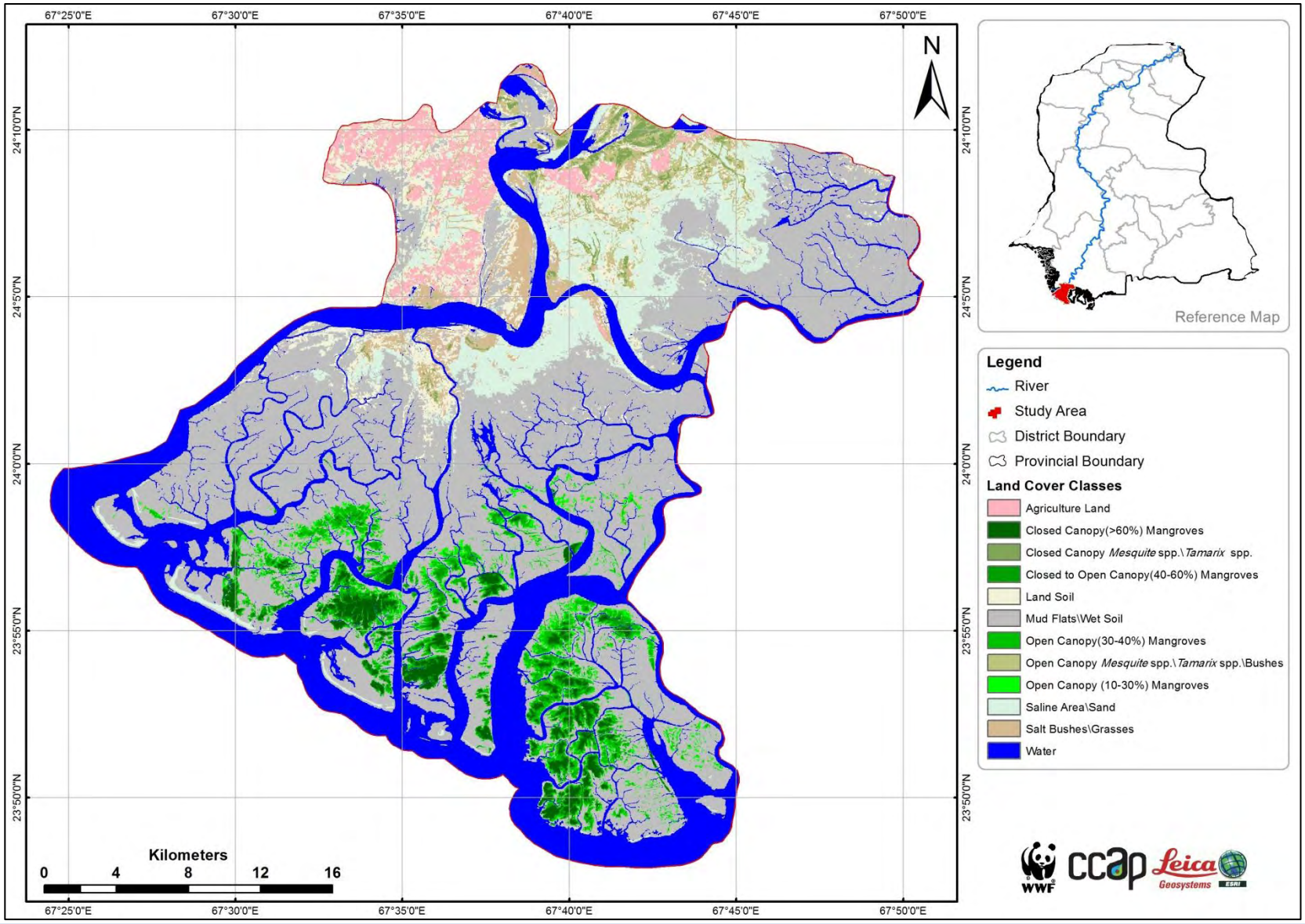

Figure 12: LCLU map of Kharo Chann developed for 2011

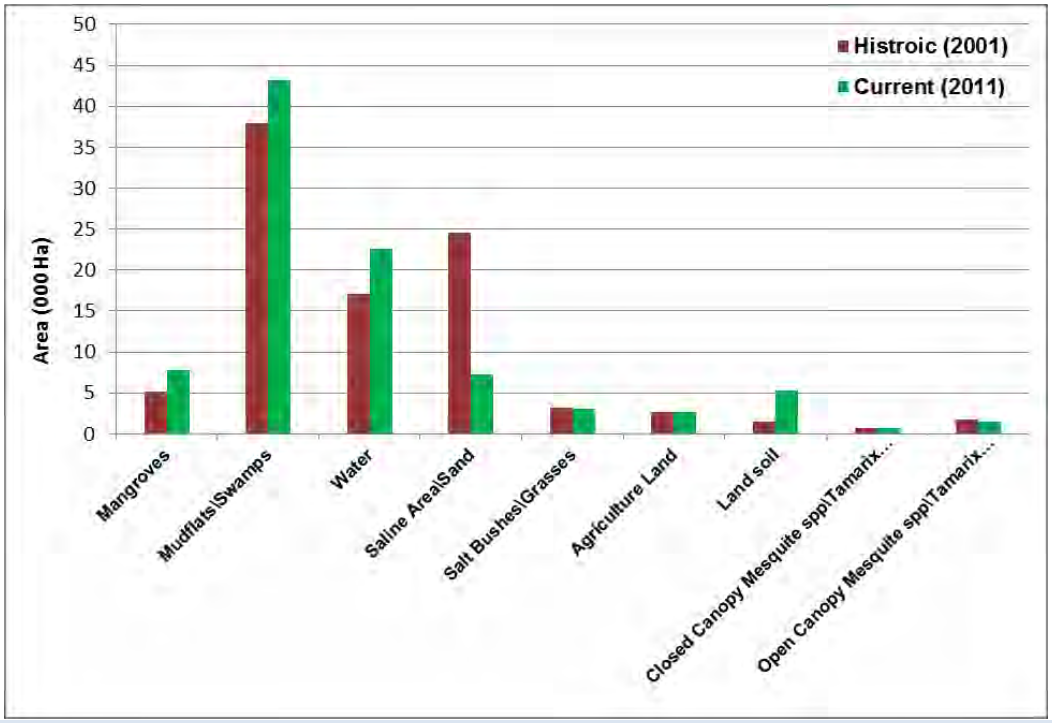

Figure 13:Graphical representation of historic and current statistics – Kharo Chann

5.3 Change Analysis of Jiwani

5.3.1 Land cover derived from 2000 satellite data

Based on Aster image of 2000, the mangrove canopy cover analysis shows that the total mangrove cover in the area was about 109 ha. Closed canopy mangroves cover was about 39 ha (35%),closed to open canopy mangrove cover was about 69 ha (63%). Mix class of Saltbush/grasses/shrubs class covers an area about 4978 ha.

5.3.2 Land cover derived from 2011 satellite data

From the analysis of Aster image of 2011, it was noted that the total mangrove cover in Jiwani is 134 ha, out of which closed canopy mangrove cover is about 71 ha (53%), closed to open canopy mangrove cover is about 63 ha (47%), Mix class of salt bushes/grasses/shrubs is spread over the area of 6,712 ha.

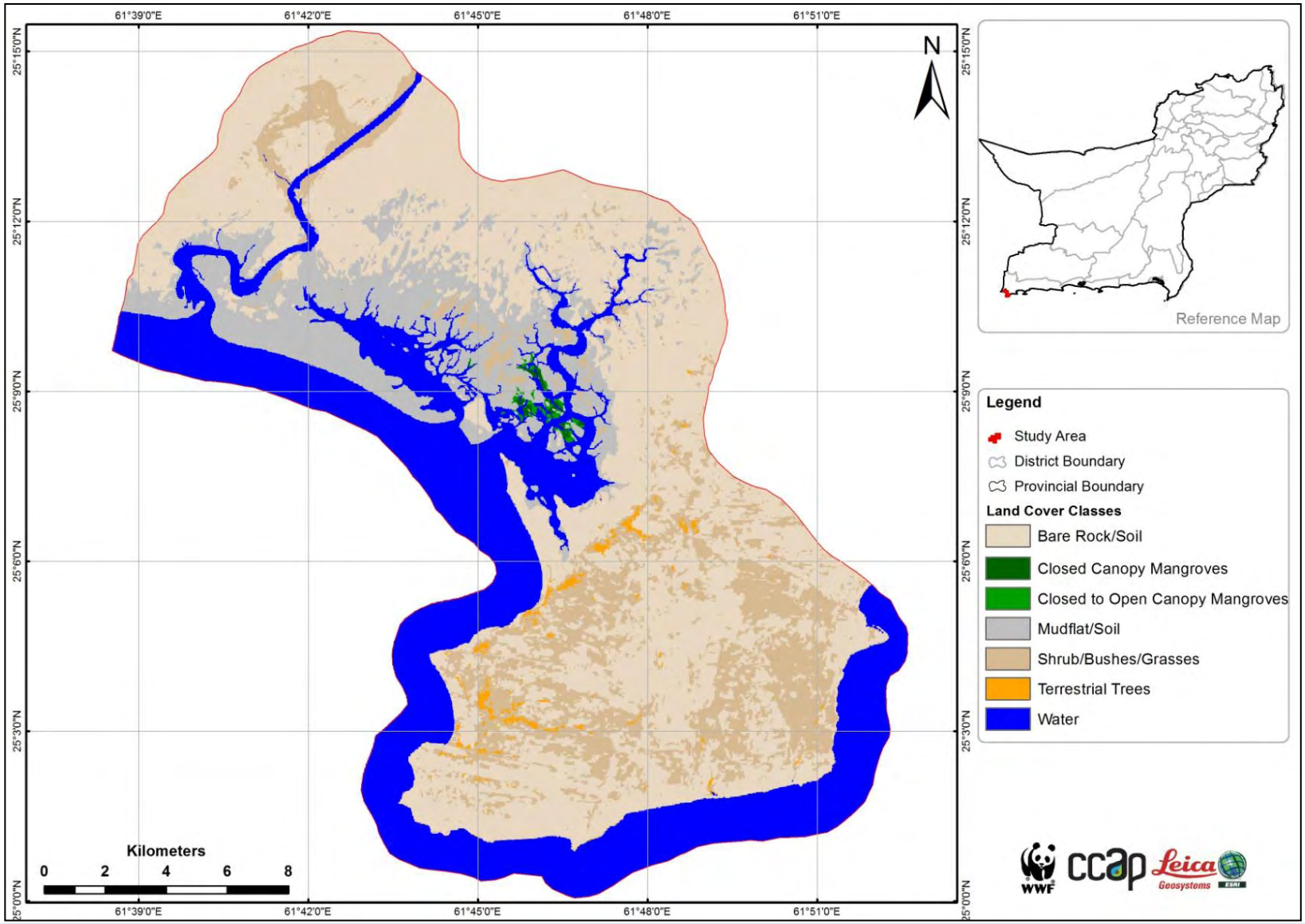

Figure 14: LCLU map of Jiwani developed for year 2000

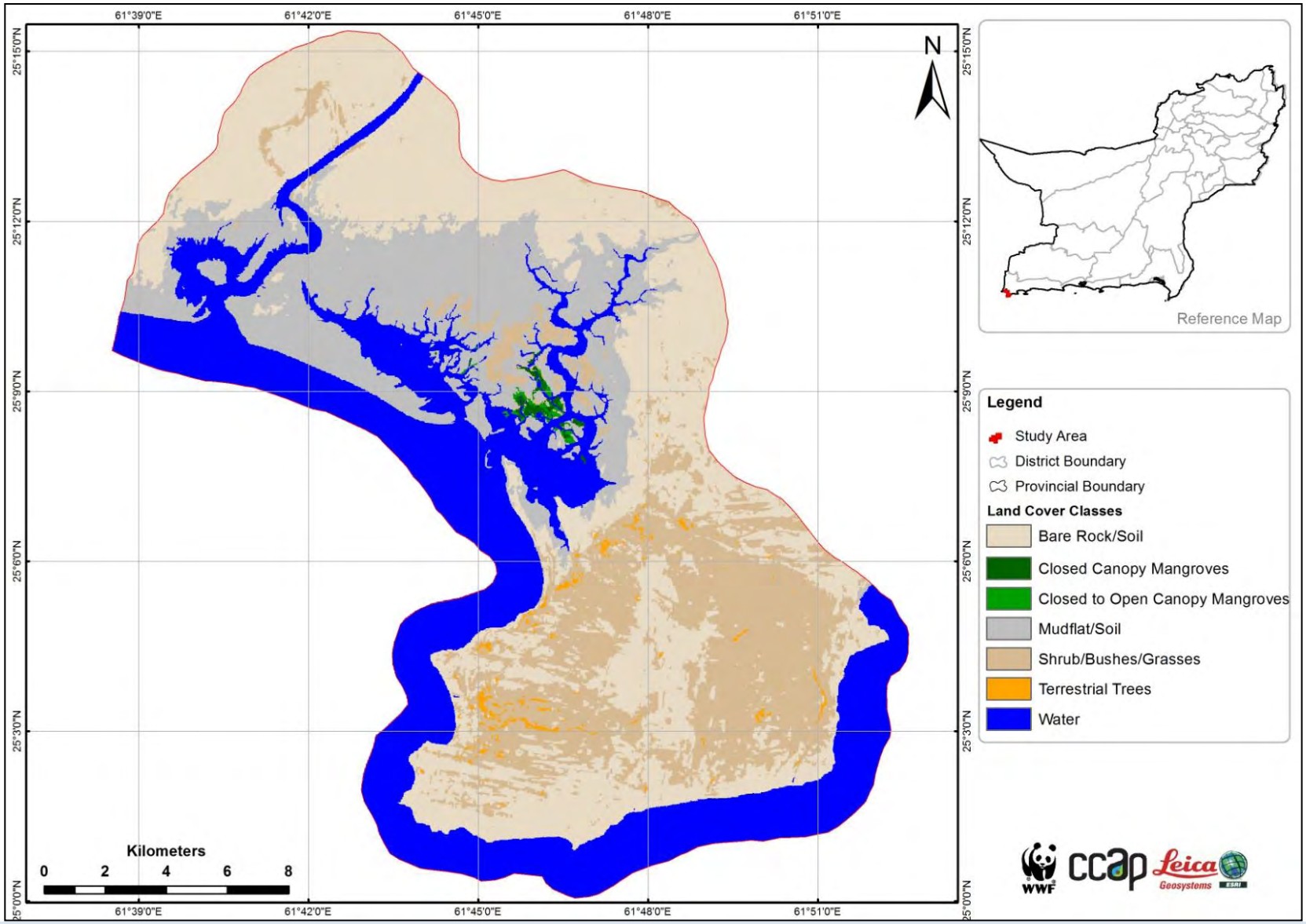

Figure 15: LCLU map of Jiwani developed for year 2011

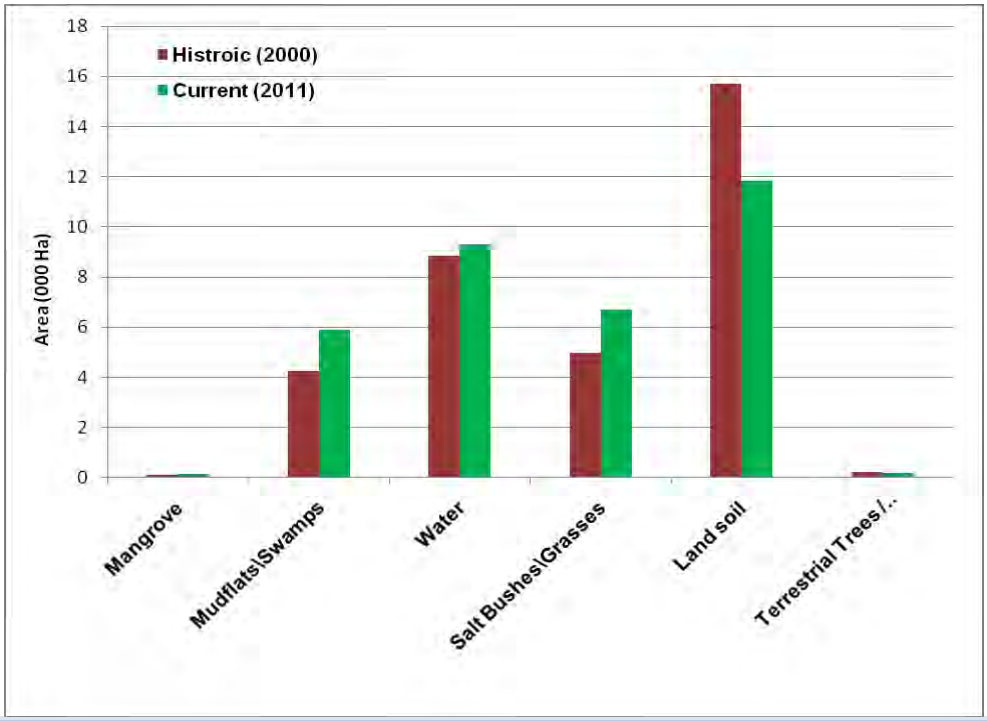

Figure 16: Graphical representation of historic and current statistics – Jiwani

Table2:Statistical details and percentage change of each class in each project site

Land Cover / Land Use Classes	Area (ha)						Percentage Change		
	Keti Bunder		Kharo Chann		Jiwani		Keti Bunder	Kharo Chann	Jiwani
	Historic	Current	Historic	Current	Historic	Current			
Closed Canopy Mangroves	1,529.19	1,628.80	1,523.16	1,956.49	39.74	71.15	6.51	28.45	79.04
Closed to Open Canopy Mangroves	1,282.14	1,467.32	773.28	1,197.16	68.94	63.54	14.44	54.82	-7.83
Open Canopy Mangroves	2,737.94	2,988.90	1,729.44	2,710.96	0	0	9.17	56.75	0
Open Canopy (10-30%) Mangroves	1,985.90	1,689.35	1,158.48	1,887.86	0	0	-14.93	62.96	0
Mudflats\Swamps	41,583.62	40,298.90	37,879.20	43,126.81	4,249.08	5,914.04	-3.09	13.85	39.18
Water	20,722.05	27,432.63	17,058.24	22,642.25	8,849.97	9,320.00	32.38	32.73	5.31
Saline Area\Sand	8,754.66	2,575.40	24,579.36	7,259.29			-70.58	-70.47	0
Salt Bushes\Grasses	574.02	1,938.92	3,165.12	3,121.92	4,978.31	6,712.58	237.78	-1.36	34.84
Agriculture Land	0	0	2,617.56	2,719.35	0	0	0	3.89	0
Land soil	0	0	1,554.12	5,268.17	15,713.06	11,836.51	0	238.98	-24.67
Closed Canopy *Mesquite*spp*Tamarix* spp.\Bushes	0	0	744.84	673.02	0	0	0	-9.64	0
Open Canopy *Mesquite* spp*Tamarix*spp\Bushes	0	0	1,793.88	1,491.14	0	0	0	-16.88	0
Buildup Area	131.99	288.43	0	0	0	0	118.52	0	0
Algal Mat	1,158.44	159.1	0	0	0	0	-86.27	0	0
Terrestrial Trees/Vegetation	0	0	0	0	220.12	201.4	0	0	-8.5

5.4 Change slices in the forested areas of Project Areas

The results reveal significant increase in the forest area of all the three project sites i.e. Kharo Chann, Keti Bunder and Jewani. In Keti Bunder, the increase in the forest cover seems to be the result of plantation activities while in Kharo Chann the patterns of plantations as well as natural regeneration have been observed. Similarly positive trend in forest cover has been assessed in Jewani area. The satellite image based slices are shown below to show the changes in selected areas;

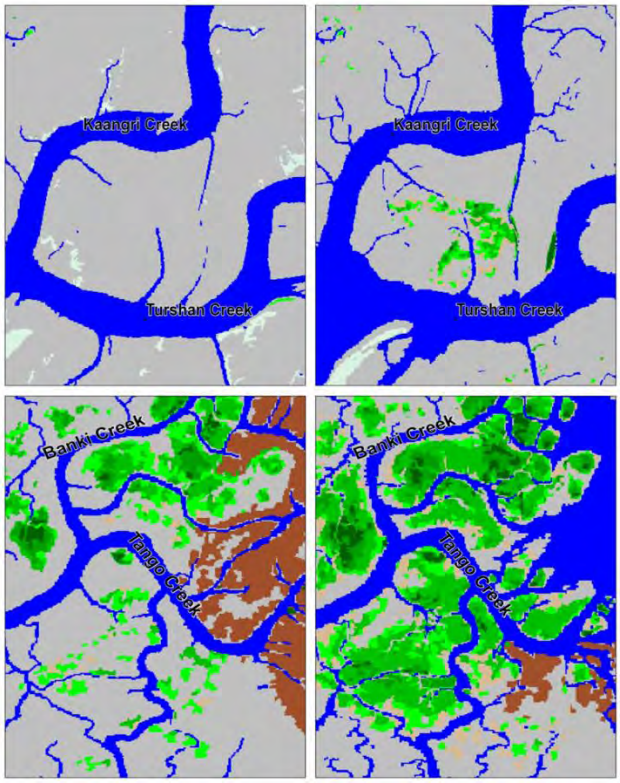

Figure 17: Increase near Turshan and Tango Creek – Keti Bunder

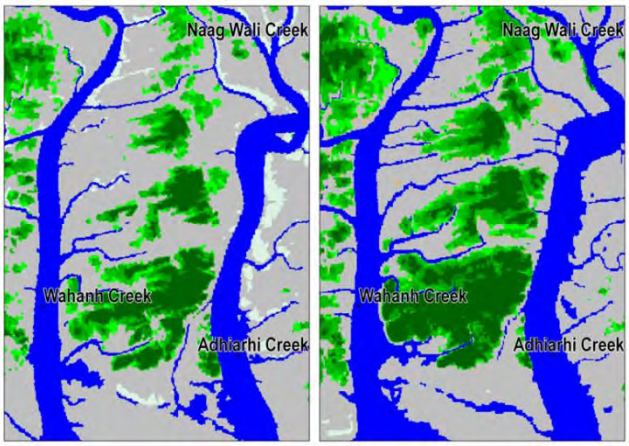

Figure 18: Increase in mangroves cover near Adhiari and Sohnri creek – Kharo Chann

Figure 19: Google earth image slice of plantation site (a) 2006 (b) 2012

Figure 20:Ground picture taken through Fixed Point Photography of mangroves plantation site in Keti Bunder – left (May 2010) and right (May 2012)

6 Hazard Mapping

Hazard may be defined as "an event or physical condition that hasthe potential to cause fatalities, injuries, property damage, infrastructure damage, agricultural loss,damage to the environment, interruption of business, or other types of harm or loss." (James & Wright, 2008)

6.1 Identification of Hazards in Study Area

Hazard identification is the process of defining and describing a hazard, including its physical characteristics, magnitude and severity, probability and frequency, causative factors, and locations or areas affected.(James & Wright, 2008). Several natural hazards has been reported in the study area over the past decade such as cyclone,floods, land erosion etc.

6.2 Cyclone

Cyclones are one of the most destructive weather phenomena, which cause innumerable damages to human lives and infrastructure across the globe. There are two major Tropical cyclone (TC) seasons pre-monsoon (April-June) and post-monsoon (October-November) as far as the Bay of Bengal and the Arabian Sea are concerned (SMRC, 1998).

The available data reveals that Pakistan's coastal area has been affected by the TCs in the years 1895, 1902, 1907, 1948, 1964, 1985, 1999, 2001, 2007 and 2010 (source: PMD and SMRC, 1998) but data of the cyclone available from 1964 to 2010 is given below in tabular form

Table 3: Historic data (1964-2010) of TC near the coast of Pakistan

Cyclone	Date	Area	Casualties	Remarks
Cyclone Phet	June 2010	Karachi		Third deadliest Cyclone in history of Pakistan, about 2 million affectless
Cyclone Yemyin	21-26June 2007	Karachi, Ormara and Pasni	700	Third deadliest Cyclone in history of Pakistan, about 2 million affectless
Cyclon TC 01A	21-29 May 2001			
Cyclone TC 02A 1999 (Category 3)	20 May 1999	Shah Bunder& Karachi	6200	Strongest and most powerful cyclone in history of Pakistan
1993 Pak-Indo cyclone (Category 1)	1993	Karachi, Thatta and Badin	609	Caused flooding and landfall in Karachi and displaced some 200,000 in Thatta and Badin
1965 Karachi Cyclone	15 December1965	Karachi Coast	10,000	Deadliest Tropical Storm in Pakistan History
1964 Indus valley cyclone	12 June 1964	Tharparkar and Hyderabad	450	Caused landfall in Tharparker and Hyderabad and left about 400,000 homeless

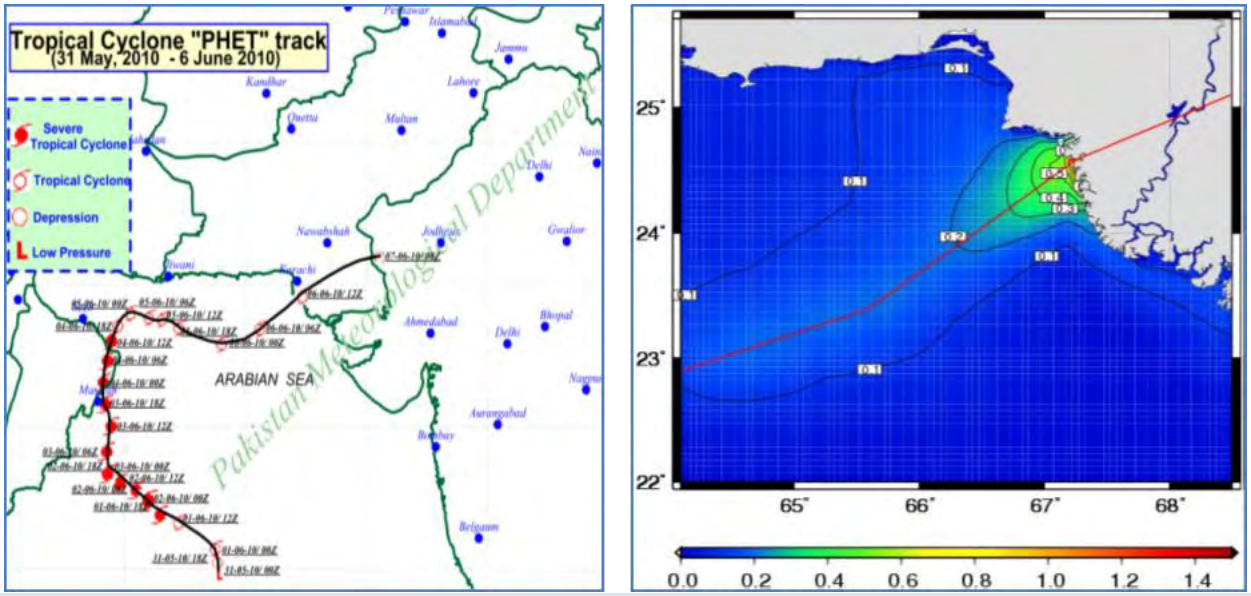

Figure 21: (Left) Phet track depicting its movement and intensity, year 2010 (source: TCWC-PMD) (Right) shows the model-simulated surge contours with a maximum value being 1.17 m

Cyclone/Tsunami in Gawadar District:

Three major cyclones (Yamin, Gonu and Phet) and two Tsunamis have been recorded over the past 66 years. This shows that the occurrence of these hazards is very infrequent and unpredictable. After Tsunami in 1945, three major cyclones in 2007, and 2010 hit the Makran coastal area. The intensity of Tsunami was very high. The physical damages show in the table below.

Table 4: Major Cyclones/Tsunami and their impact

Hazard	Year	Season	Geography	Physical damages (Score)	Economic and financial losses (% + Score)	Overall Impact (Sum of score)
Pishukan, PasniCyclone (Phet)	2010	6 June	Gwadar city, Jiwani, Pasni, KalaagKolanch, Nalant, Suntsar, Surbander, Pishukan, Pasni	370 mm rainfall Wind speed 60-80 km/hr Roads and sewerage systems were blocked 2-3 human Casualties and 30 injured Old city Gwadar submerged in water 90 HH damaged	4	9

				(6000-7000) 60% boats Destroyed **5**		
Cyclone (Yamyin)	2007	July 7	Suntsar, Kalag, Basur,	One week after Gonu 200 boats destroyed 17 fisherman died 24 HH damaged Disease outbreak 70% agri land damaged Coastal Highway blocked **4**	4	8
Cyclone (Gonu)	2007	June 6	Pishukan, Gwadar, Surbandar, Ormara.	CNW Rpt Fisheries Report **2**	2	4
Tsunami (Sea flood)	1945	October-Novembr	Pasni, Gwadar (Partial),	More than 8 rector scale 4000 human casualties Pasni declared red zone Gwadar declared hotline (Zone 4) All huts and Kachha houses destroyed **5**	5	10
Tsunami (Sea flood)	2009	July 7	Pasni, Gwadar (Partial),	**5**	4	9
Total				**21**	**19**	**40**

For the mapping of intensity of the Cyclone/Tsunami in Gawadar district, this tabular data was converted in the GIS layers using interpolation techniques. After the spatial interpolation, an intensity layer was generated which is based on the overall damage of the cyclone/ Tsunami in Gawader.

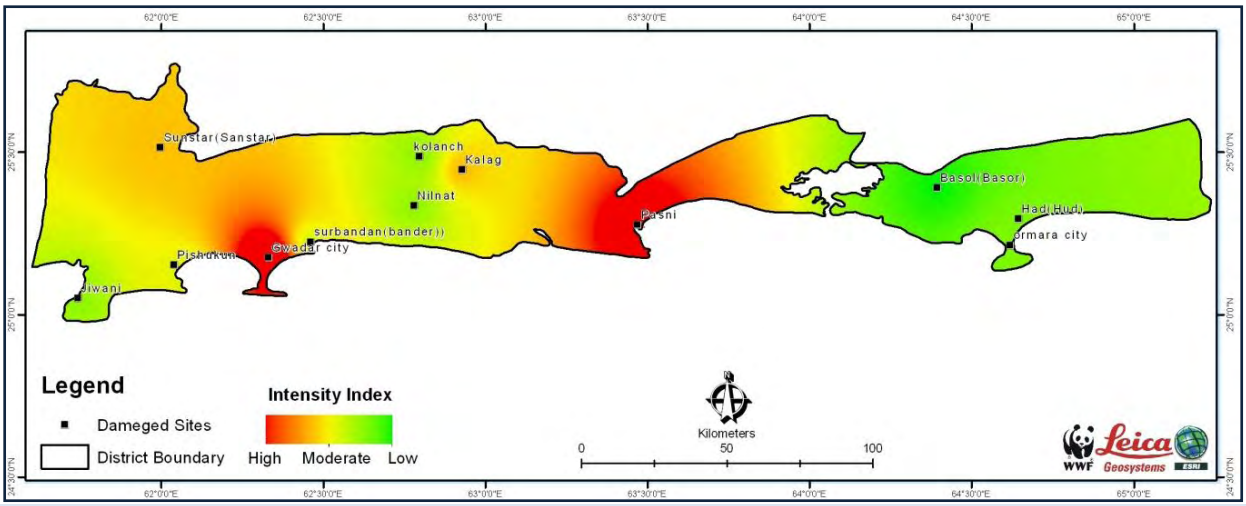

Figure 22: Intensity map of Cyclone/Tsunami of Gawadar District, Pakistan (1945-2010)

6.3 Floods in Pakistan

Flood hazard is the potential for inundation that involves risk to life, health, property, and natural floodplain resources and functions. It is comprised of three elements: severity (magnitude, duration, and extent of flooding), probability of occurrence, and speed of onset of flooding. The 2010 Pakistan Floods caused by unprecedented monsoon rainfall has resulted in disastrous impacts. Considering the number of people affected, the 2010 floods can be tagged as one of the worst natural disastersin the country and is considered as one in a hundred year event (Figure 23).

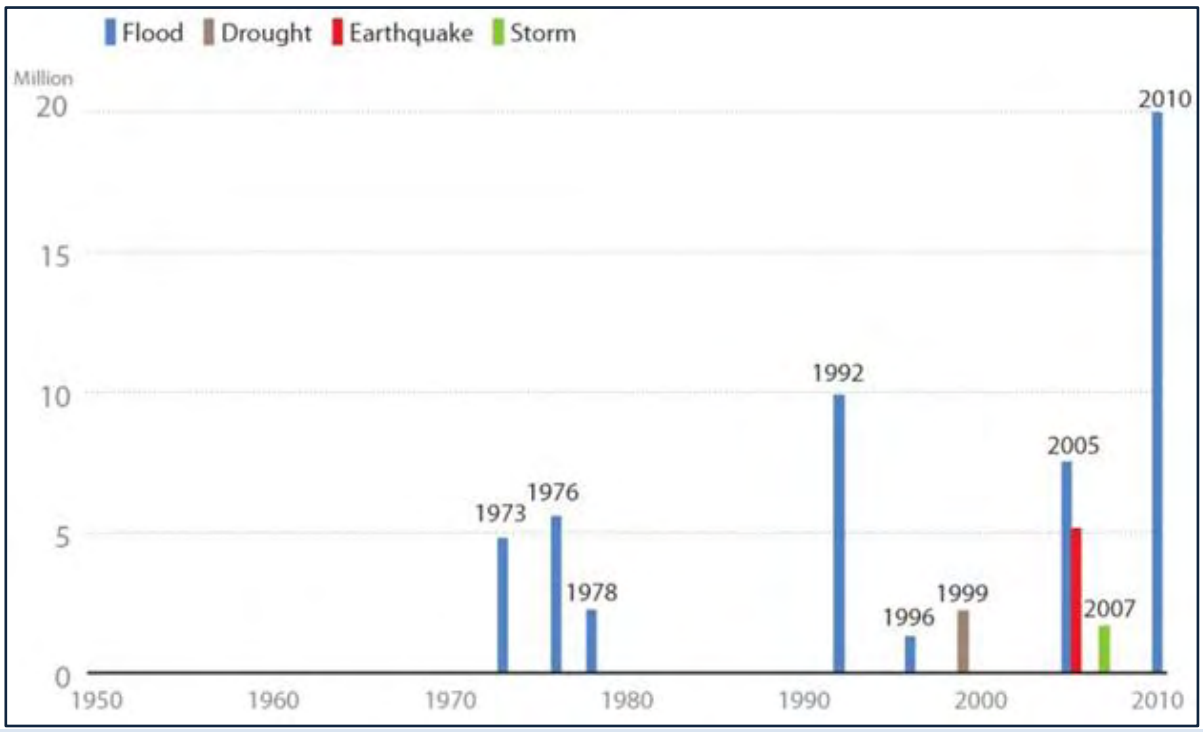

Figure 23: Ten biggest natural disasters in Pakistan (Source: UNOCHA)

The temporal images of MODIS data showing the pre and post flood extent of 2010 along the Indus River in Sindh province is shown in the figure below.

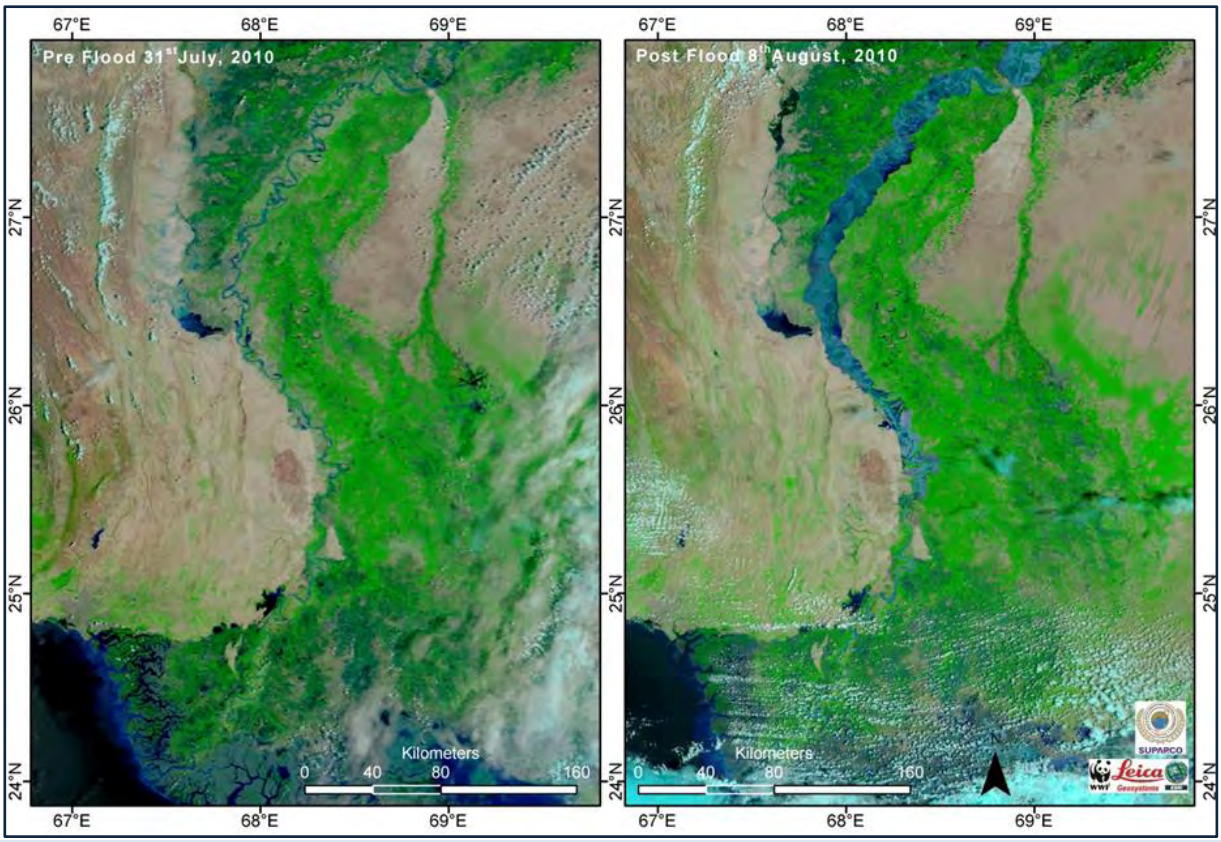

Figure 24: MODIS images - flood extent along the Indus River, Sindh

It was analyzed by comparing pre (26th March, 2010) and post (28th September, 2010) flood satellite images and the land cover maps that recent floods have resulted in land erosion in some of the areas of Kharo Chann. The land cutting due to water pressure was high near Atharki, SalehDandal, Jamnasar and ChorGoju villages (Annexure II for the geographic coordinates). Approximately an area of 38 ha has been lost around these villages during the flood period. The areas near Atharki and SalehDandal villages have been facing land erosion since year 2000 but the floods 2010 washed away some of the agricultural fields and houses as shown in Figure 25.

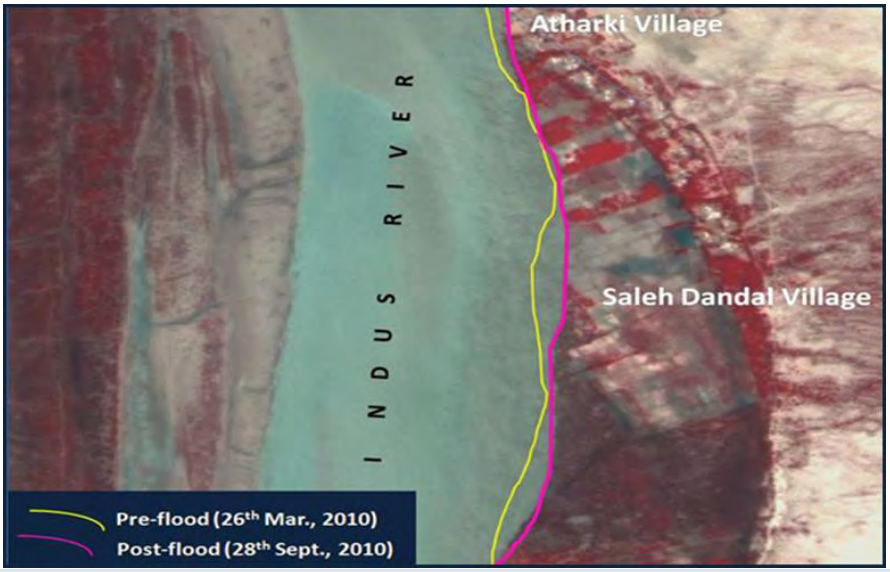

Figure 25: Erosion due to flood 2010 along Indus river in AtharkiVillage

6.3.1 *Flood Susceptibility Mapping using Logistic Regression*

Study Area

Thatta district boundary was used as an AOI for the analysis with slight modifications on the eastern boundary based upon the availability of predictor variables (Figure below)

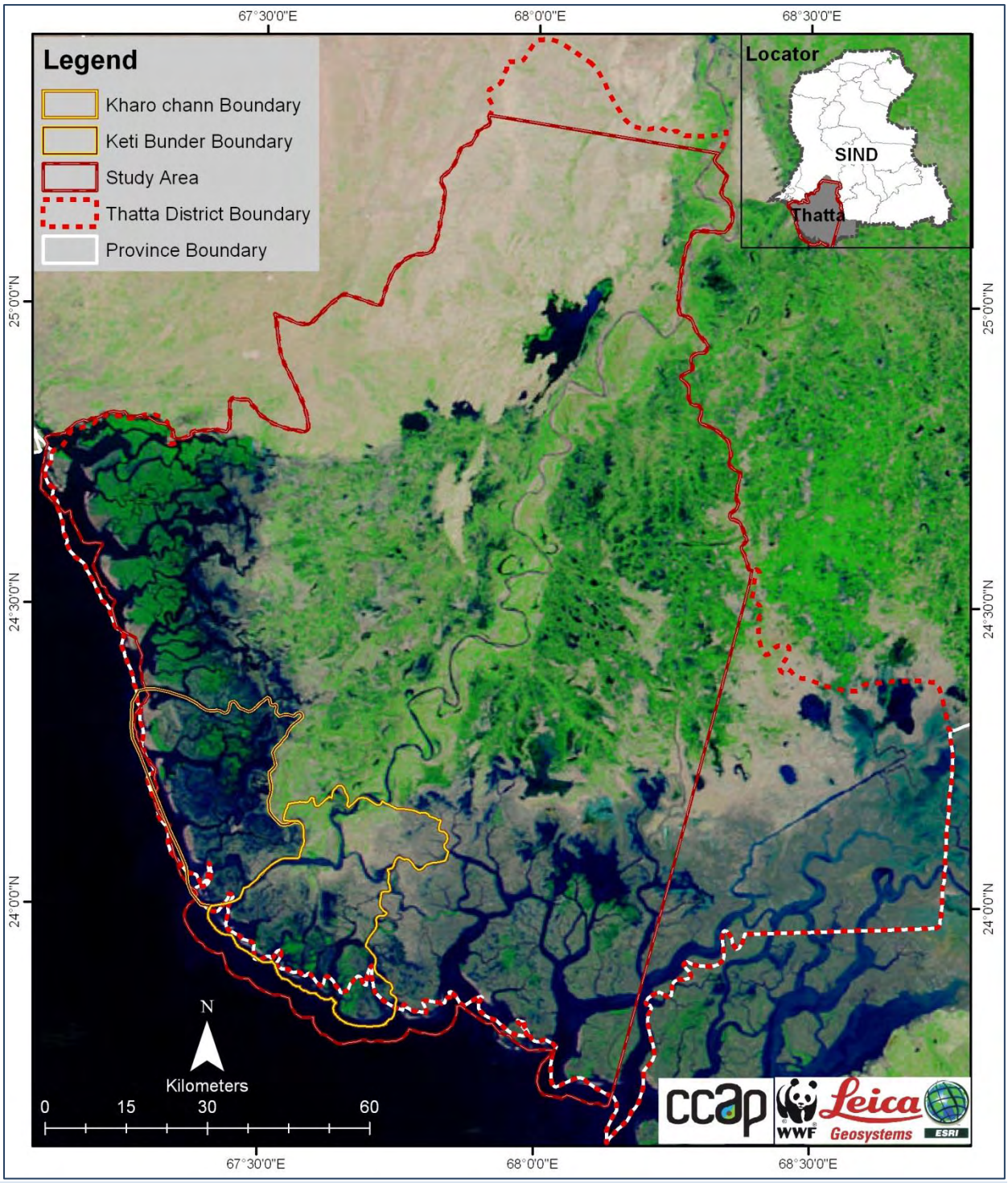

Figure 26: Map showing the AOI used for the study

Flood Data

Analysis were carried out on the point data generated data of the flooded sites of district Thatta, it was used as sample points for the predictions of potential flooded area in the district Thatta.

Predictor Variables

A wide range of input variables have been used in flood susceptibility mapping (Pradhan, 2009; Theilen-Willige, 2012). Most common are variables relating to climate (e.g. temperature, precipitation), topography (e.g., elevation, slope, aspect), soil type and land cover type (Pradhan, 2009).

Six variables (Table 5) were identified as potential predictor for flood susceptibility mapping. These variables were chosen based on their relevance to target flood mapping also used in several relevant studies (Campbell, 2001; Mckenzie et al., 2005 Theilen-Willige, 2012). A brief description of the variables is as under:

Table 5: Predictor variables used for the intensive and extensive analysis

Variable	Data format	Resolution	Data Sources
Land cover	Raster	30m	Landsat
DEM	Raster	30m	ASTER GDEM
Slope	Raster	30m	
Curvature	Raster	30m	
Pre flood Extent	Raster	30m	Landsat
Precipitation (min.)	Raster	2.5 km	Meteorological Department
Precipitation (max.)	Raster	2.5 km	

Land cover

For the current study a land cover (Figure below) was developed using pre flood LANDSAT satellite data of 30m spectral resolution.GPS based ground truth data collected during the field surveys was used as training data for land cover development and accuracy assessment.

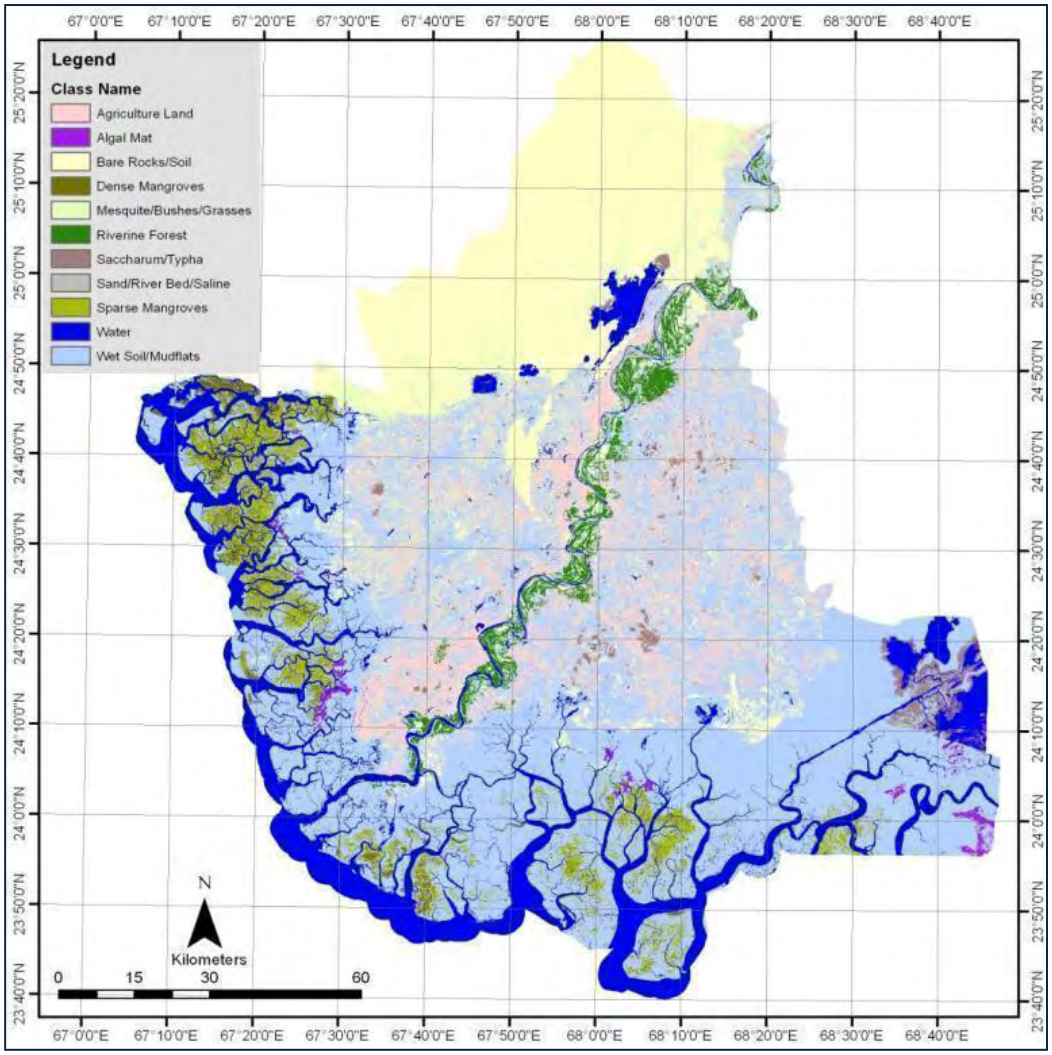

Figure 27: Map showing the land cover of the study area

Indus River and Wetlands Extent Under Normal Situation

It was derived from the LANDSAT TM satellite image using mean values of mid infrared band of the satellite data as shown in figure below.

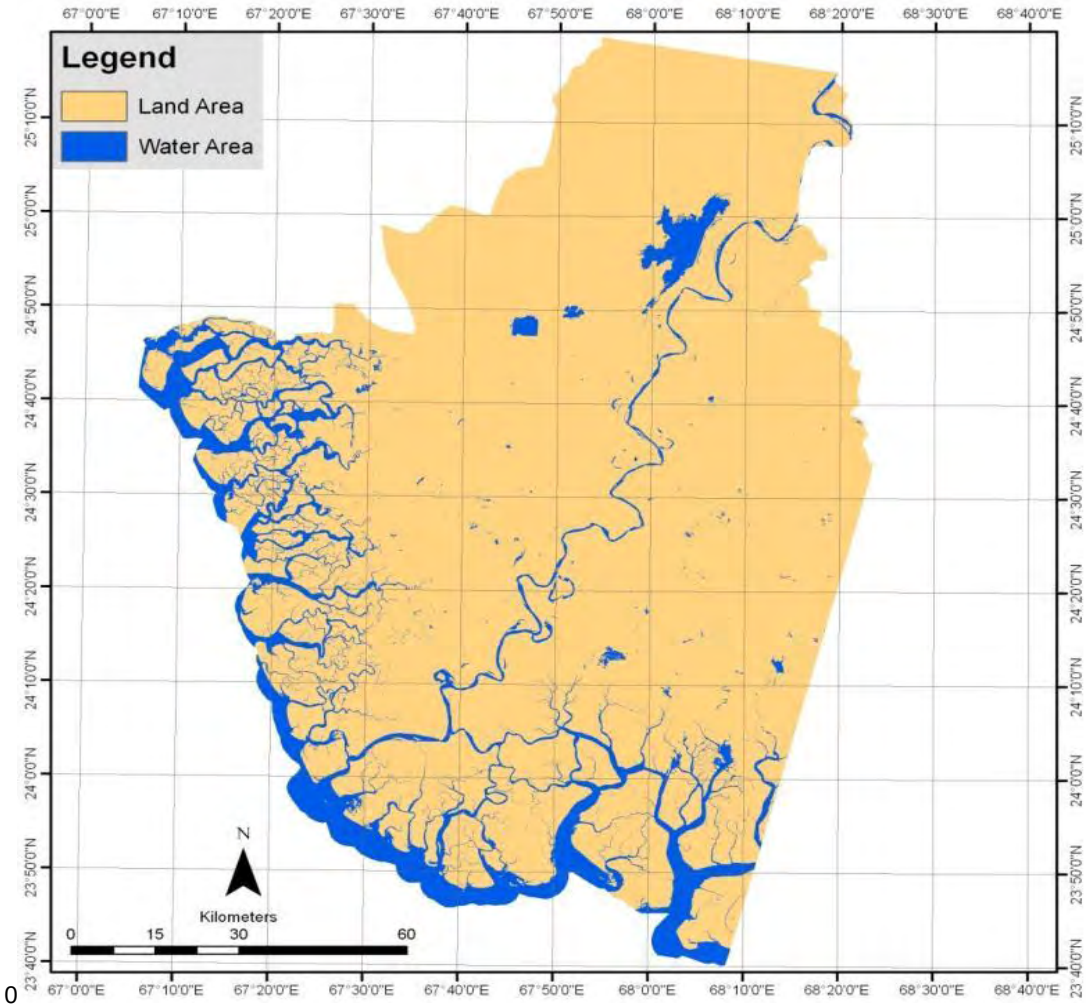

0

Figure 28: Water Extent in Normal Circumstances

Climatic Variable (Precipitation)

Moreover the climatic variable that play important role in flooding is the amount of precipitation that was acquired from Pakistan Meteorological Department (PMD). The records averaged out and min/max were calculated on annual basis.

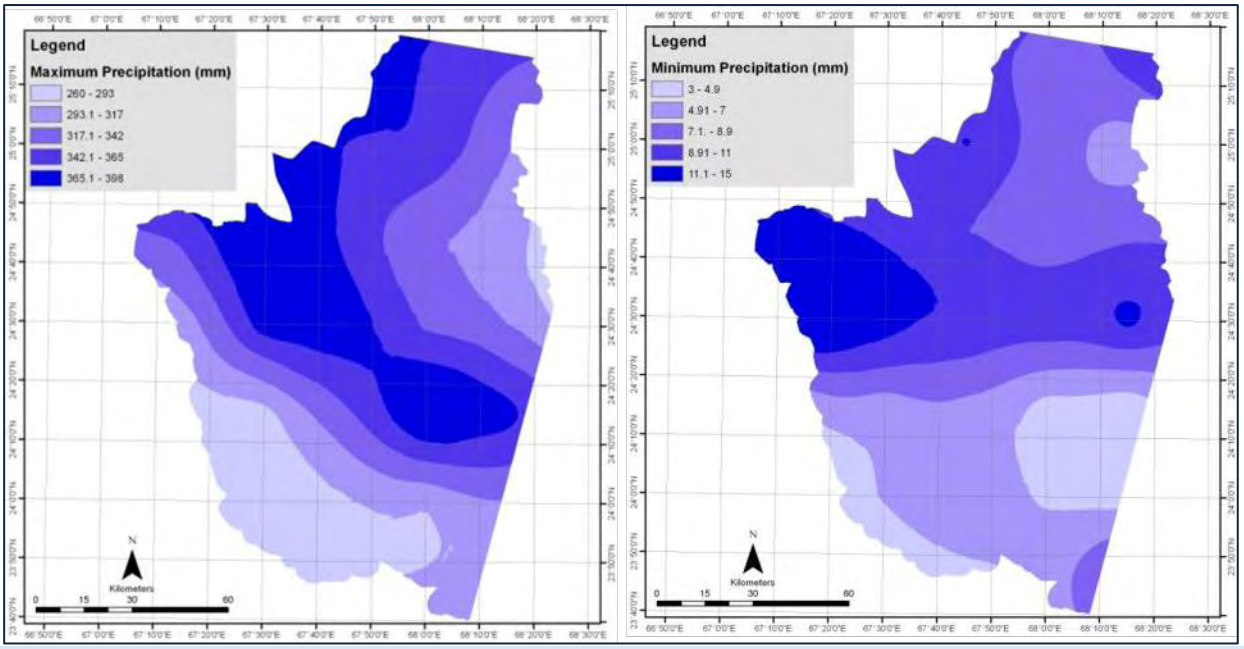

Figure 29: Precipitation layers for the minimum and maximum values for past 30 years

Topographic Variables (DEM, Slope, Curvature)

ASTER (Advanced Spaceborne Thermal Emission and Reflection Radiometer) digital elevation model (DEM) with a spatial resolution of 30m was used as elevation data for the study (Figure 30). It was downloaded from ASTER GDEM website (http://www.gdem.aster.ersdac.or.jp/). Slope and curvature layers (Figure 17) were derived from the DEM data layer using surface analysis tool of the spatial analyst in ArcGIS 9.3®. The DEM slope and curvature were further clipped and resampled on the study area boundaries and were converted to ASCII format to be used in the modelling software.

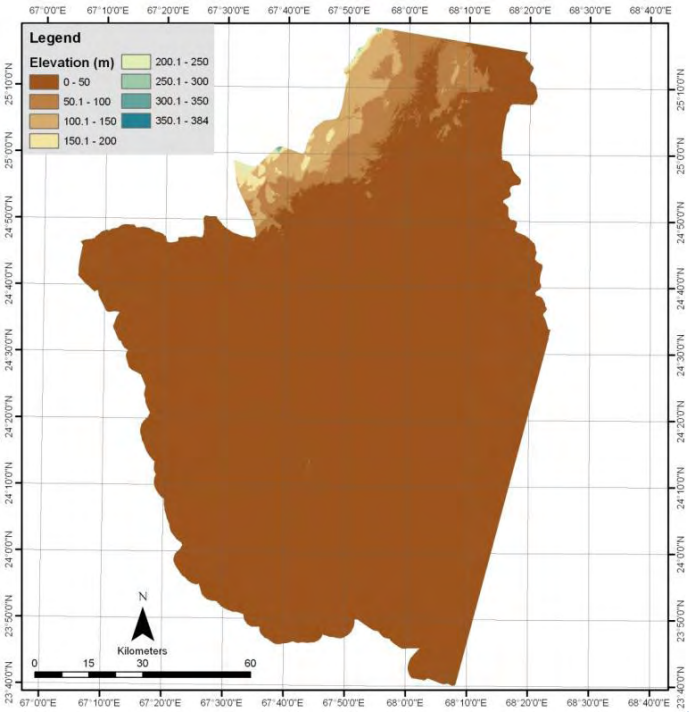

Figure 30: ASTER GDEM of 30m resolution for the study area

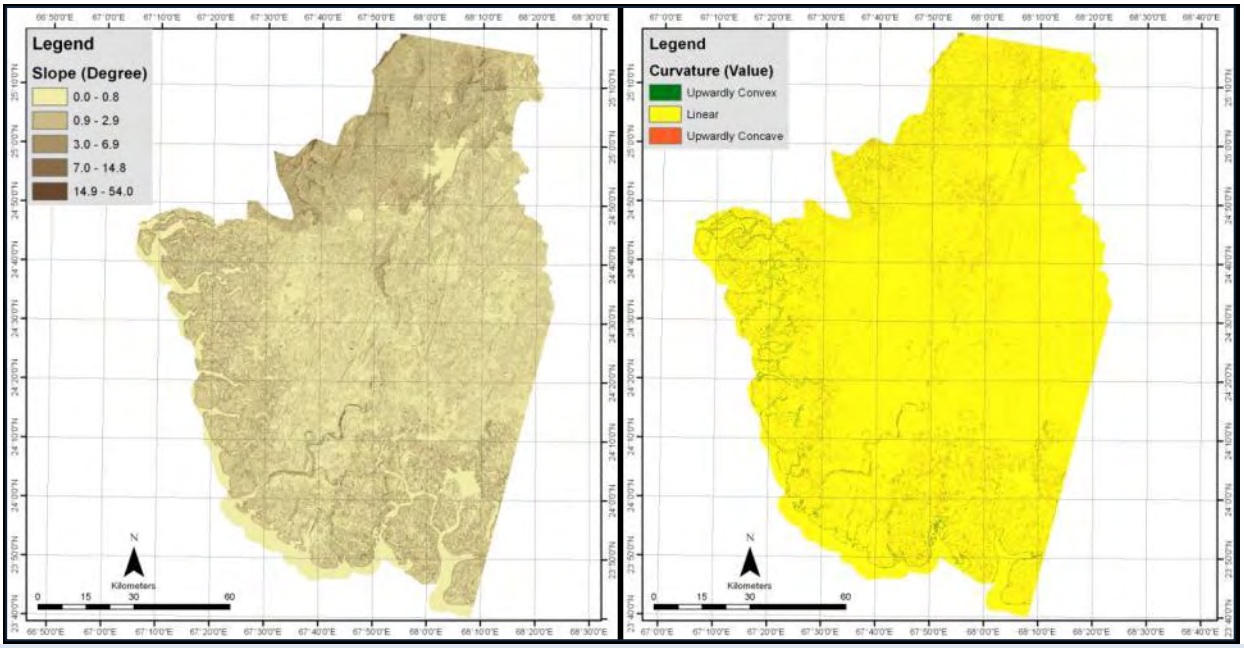

Figure 31: Slope and curvature maps derived from ASTER DEM

Modeling Approach

Flood susceptibility mapping using GIS, logistic regression and neural network methods have been applied in various case studies (Zerger, 2002; Sanyal and Lu, 2004; Knebl et al., 2005; Pradhan, 2009). Logistic regression allows one to form a multivariate regression relation between a dependent variable and several independent variables. Logistic regression, which is one of the multivariate analysis models, is useful for predicting the presence or absence of a characteristic or outcome based on values of a set of predictor variables. The advantage of logistic regression is that, through the addition of an appropriate link function to the usual linear regression model, the variables may be either continuous or discrete, or any combination of both types and they do not necessarily have normal distributions. In the case of multi-regression analysis, the factors must be numerical, and in the case of a similar statistical model, discriminant analysis, the variables must have a normal distribution. (Atkinson and Massari, 1998).

Current study is based on remote sensing data along with other climatic data for the flood susceptibility mapping for part of Thatta district majorly covering the Indus Delta. Terrain information such as DEM, slope, curvature, distance from drainage, flow direction, flow accumulation, land cover and precipitation information have been updated to enable the quantification of flood associated attributes. Flood susceptibility mapping has been applied using logistic regression in MAXENT model. Further analysis was carried out using the output from the flood susceptibility analysis and the socio-economic parameters in GIS environment.

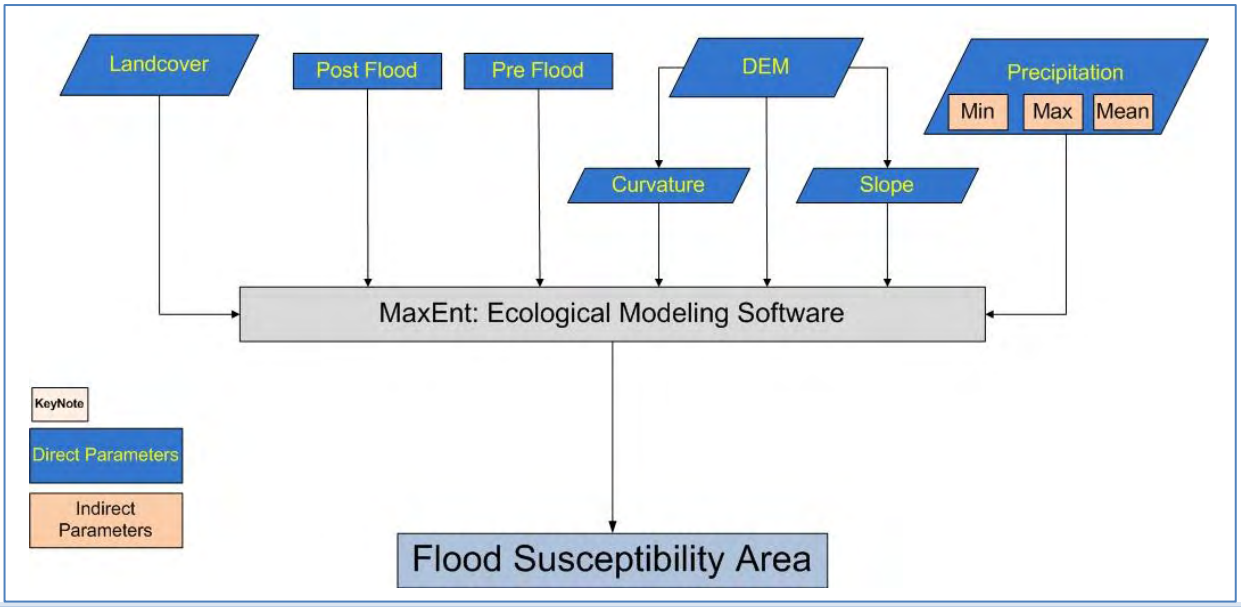

Figure 32: Flow diagram of the flood modeling

Outputs

Output is mainly divided into three parts viz., generalized, with minimum precipitation and with maximum precipitation.

Figures below show the flood susceptibility areas in raw as indicated in the aforementioned cases.

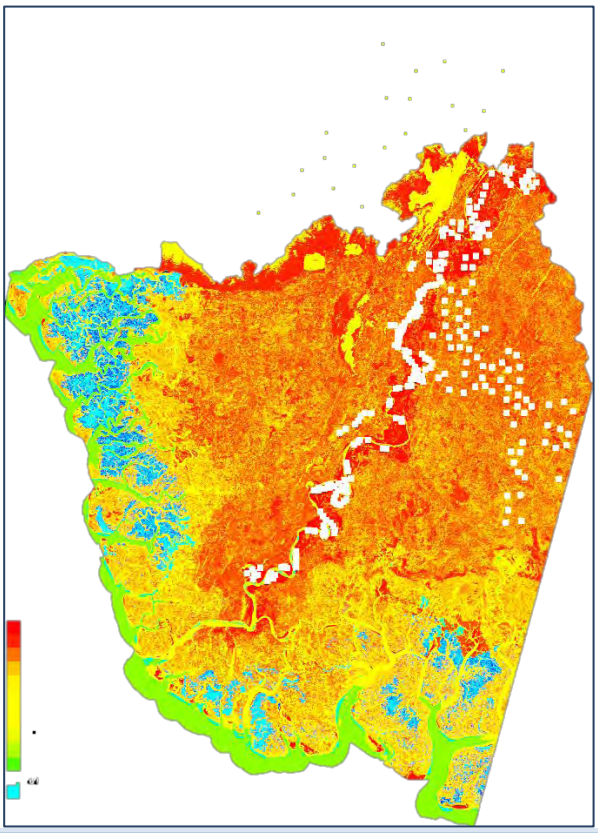

Figure 33: Direct output for flood susceptible area without precipitation

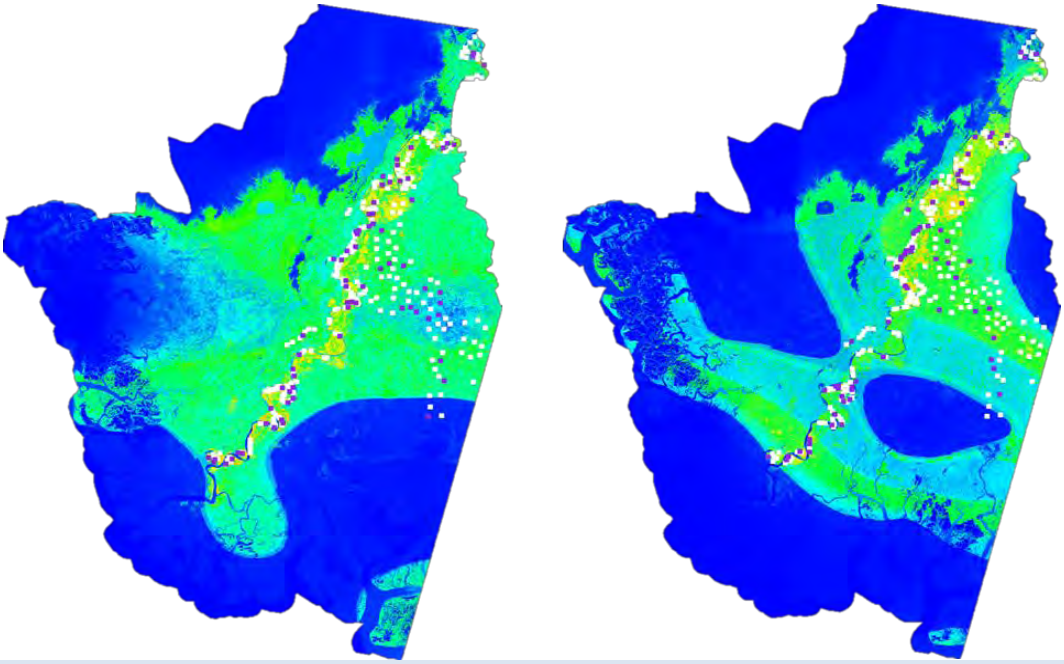

Figure 34: Flood susceptible areas direct output for minimum precipitation (Left) and for maximum precipitation (Right)

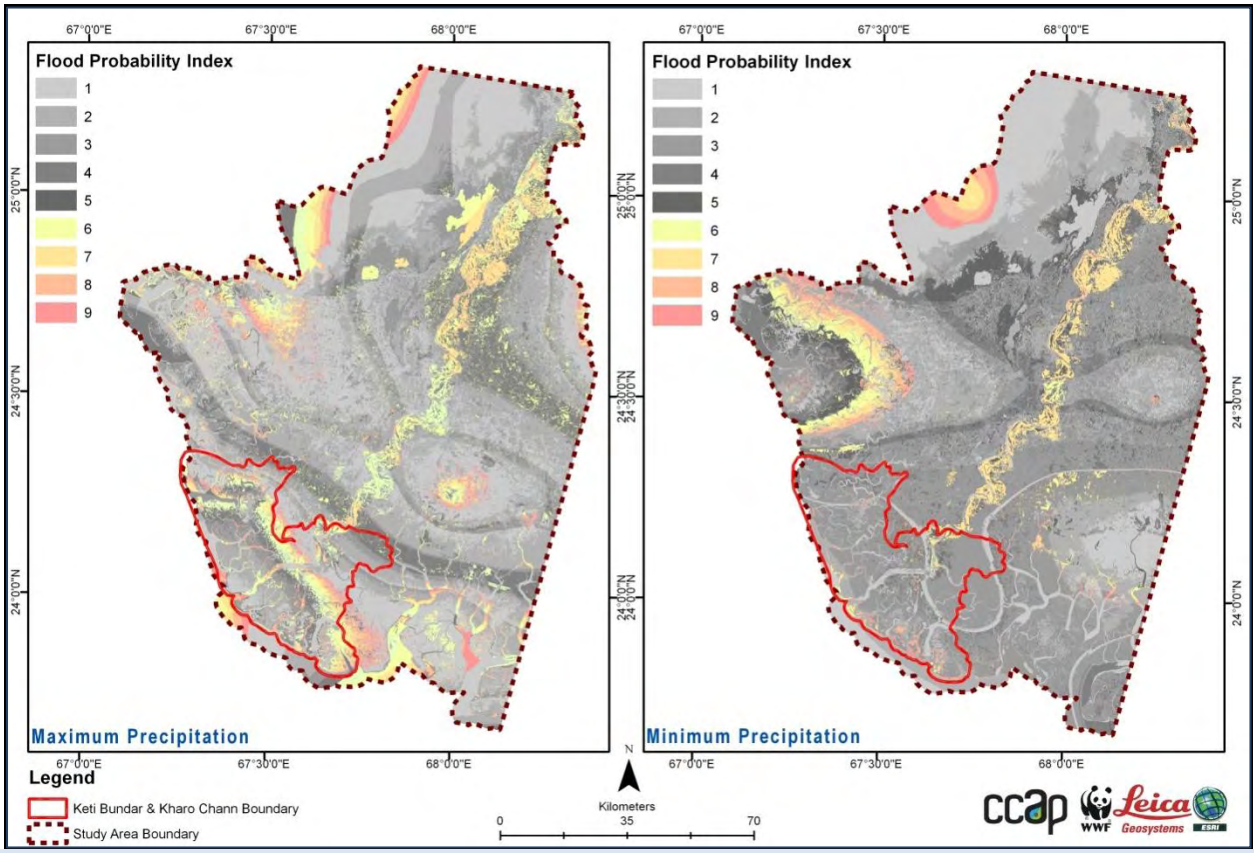

Figure 35: Flood susceptibility for different precipitation scenarios

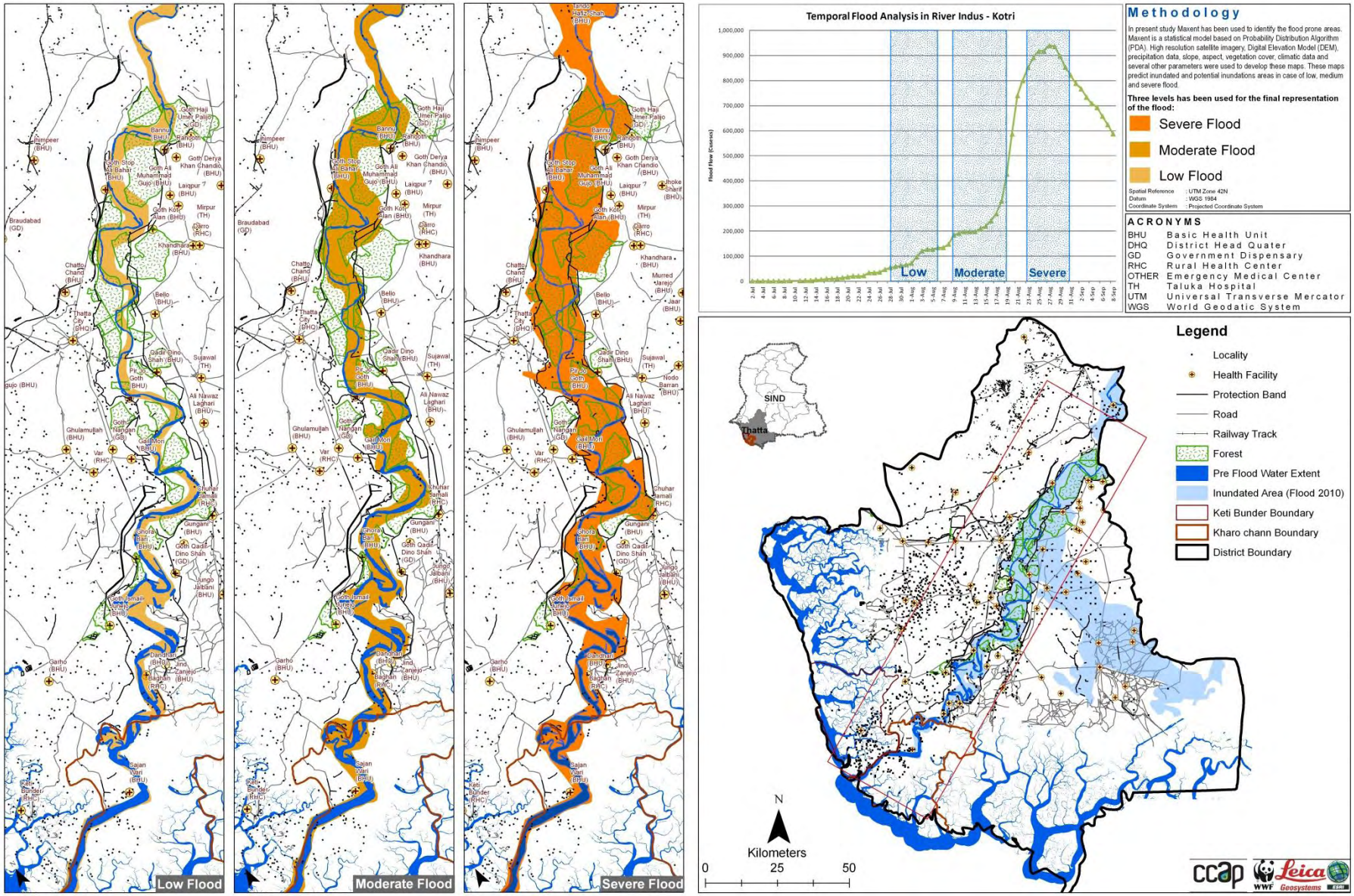

Figure 36: Map showing flood prediction estimated at three levels for Thatta district

6.4 Land Erosion/Accretion

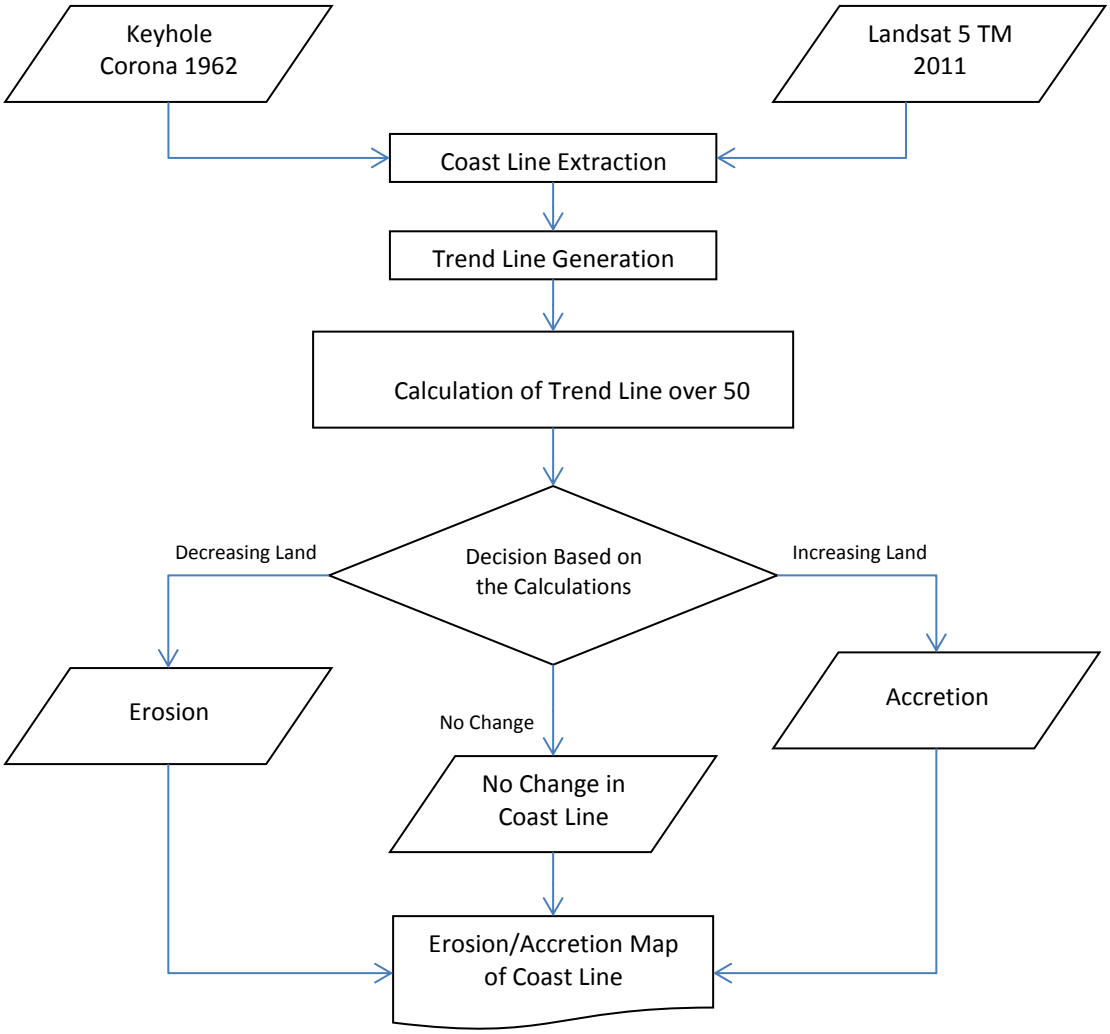

Figure 37: Erosion / Accretion change flow chart

Land erosion due to sea water is another factor affecting the loss of land in coastal areas. The primary reasons of shoreline/coastline erosion are the currents and wavesactions of the sea which is a continuous phenomenon spread over centuries. However, the sea level is rising and it appears as one of the cause of catalysing the erosion process.To analyse the balances between the land loss and gain, historic datasets of Corona (Keyhole) 1962 was compared with the Landsat satellite image of June 2011. Theresults revealed an erosion of approximately 9,065 ha of land in Keti Bunder and Kharo Chann whereas only 1,347 ha of land have been accreted along the shore line. The trends of shrinking and expanding land masses were used to calculate rate of land erosion/accretion for 49 years(Figure 38, 39).

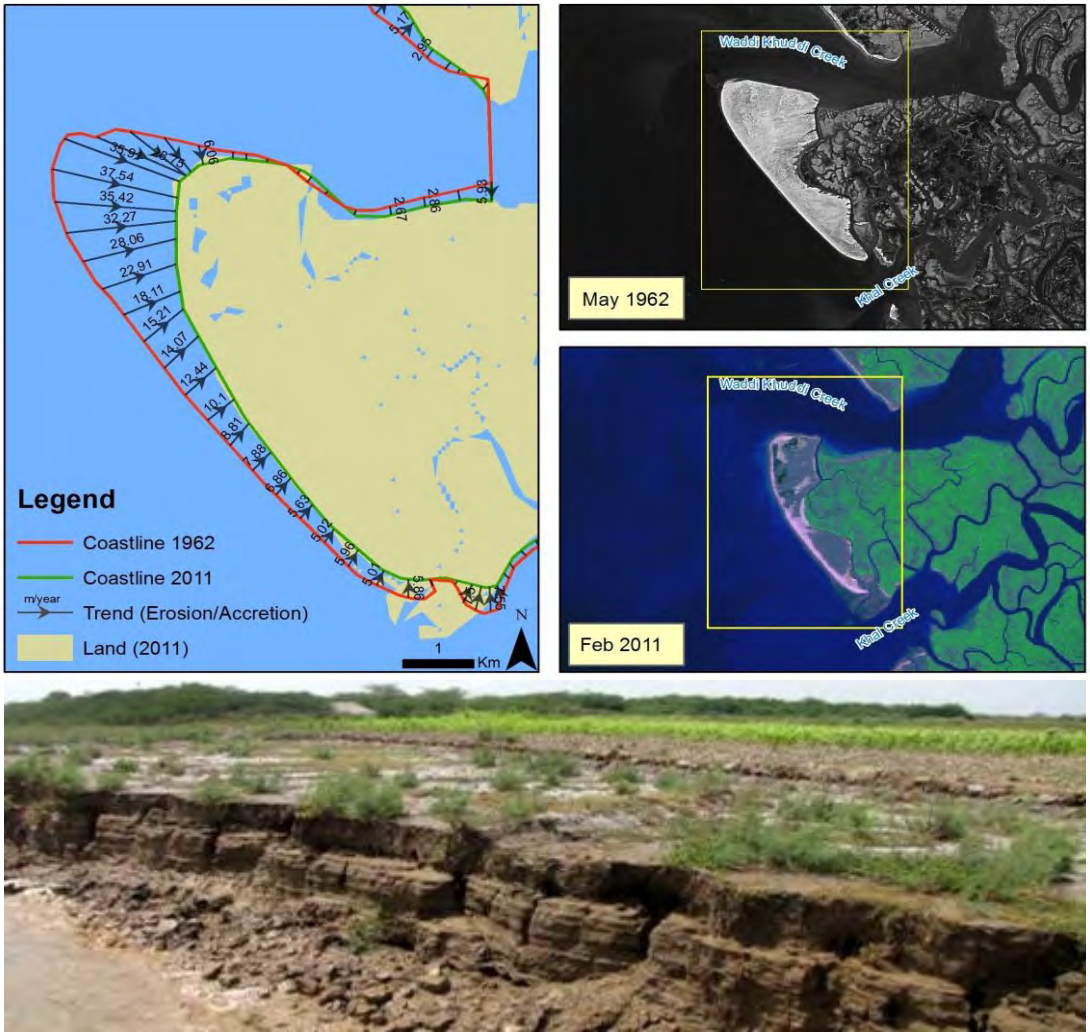

Figure 38: Near WaddiKhuddi Creek, red line shows the position of coastline in 1962 and the current position in 2011 is in green colour. Trend line highlights erosion of the land in meters.

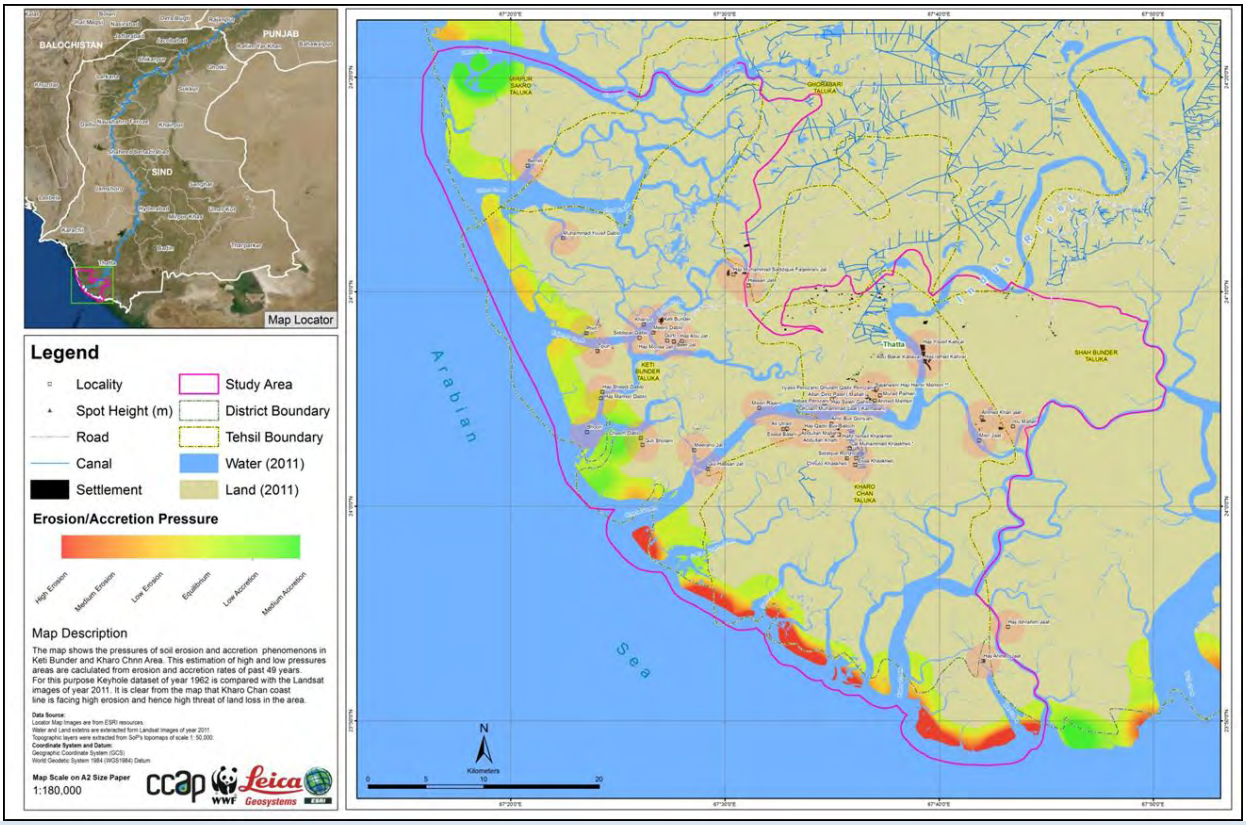

Figure 39: Density Map - Erosion and Accretion Pressure (Keti Bunder and Kharo Chann)

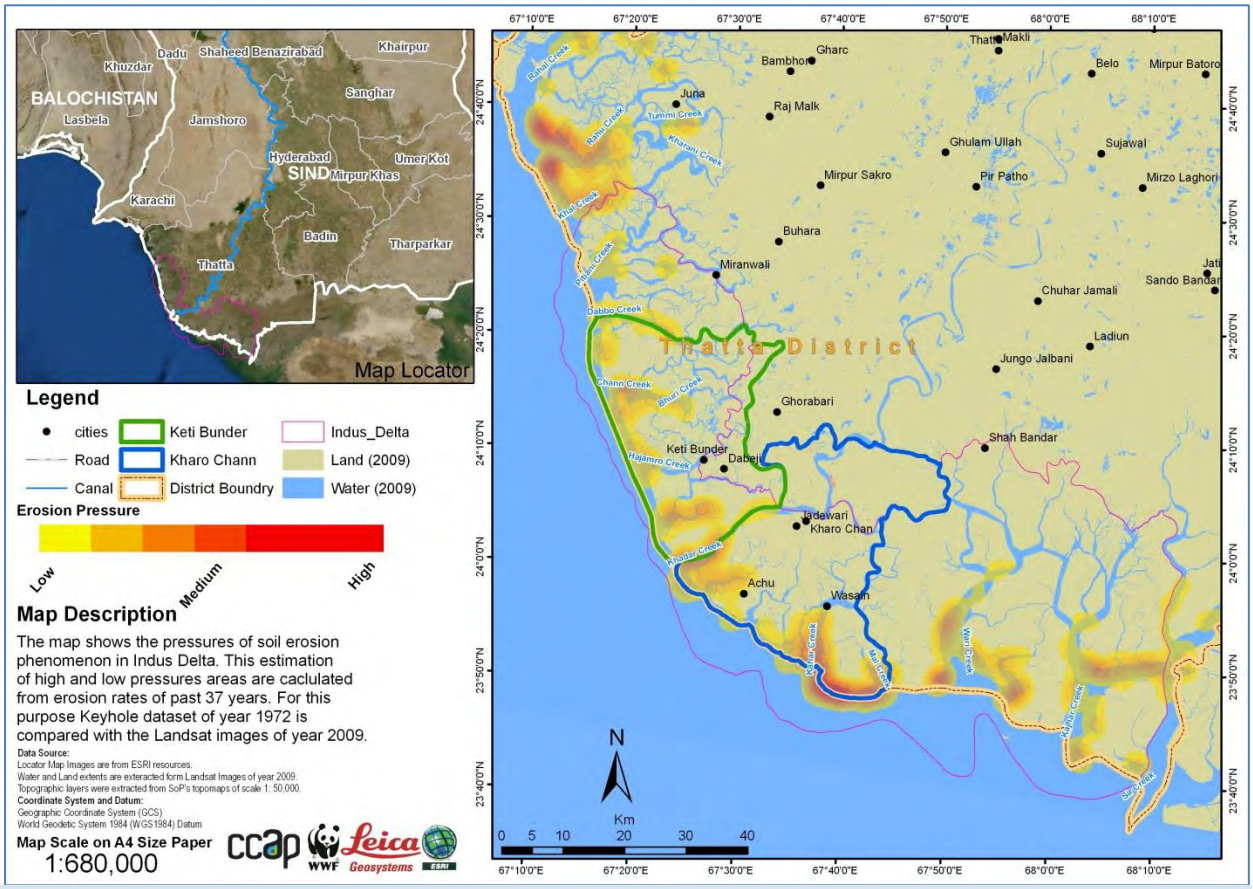

Figure 40: Overall soil erosion pressure areas in indus delta

Inland Deltaic Extent Change Pattern

The images were interpreted to extract the Indus Delta inland extent. The change pattern shows that the sea water is intruding and resulted in land damage due to increased salinity hence deterioration of agricultural land (Figure 41).

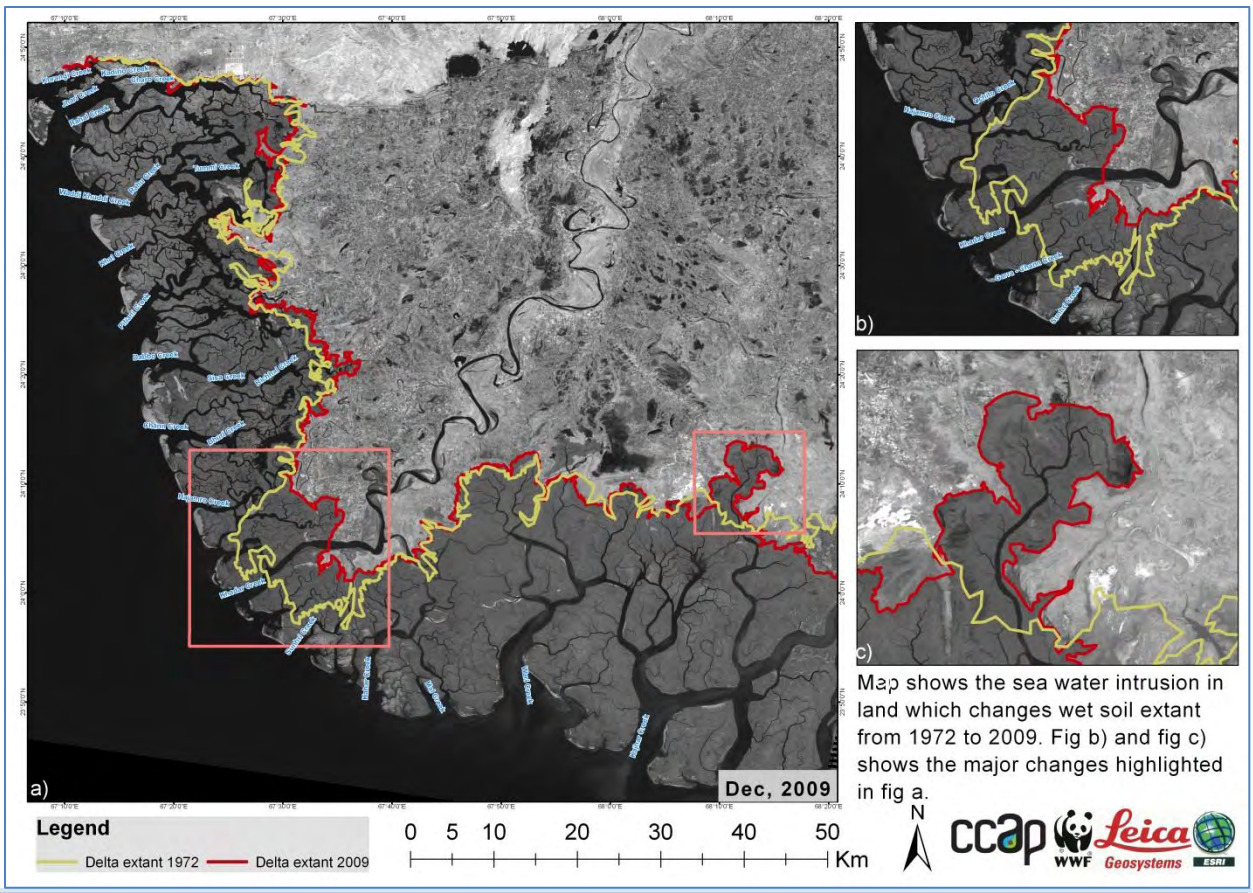

Figure 41: Inland deltaic extent of Indus delta

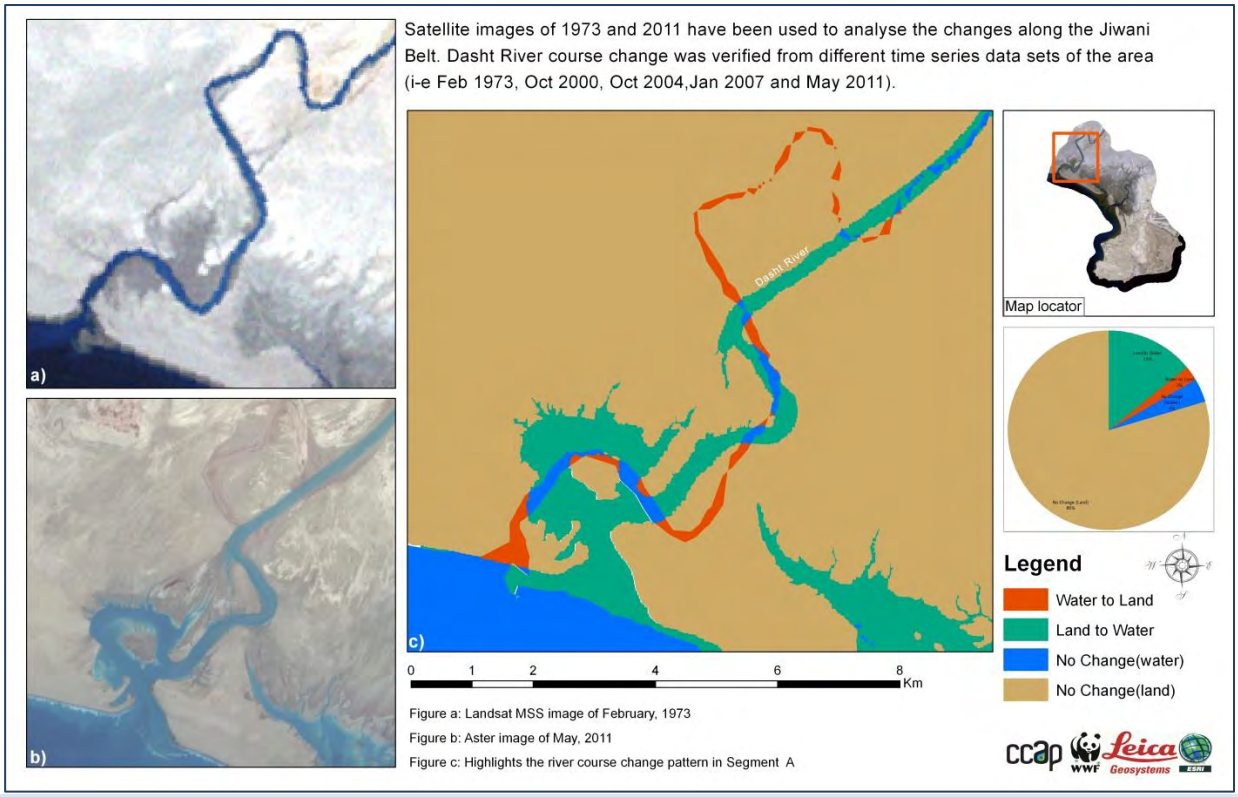

Figure 42: A remarkable erosion and accretion, observed along the coastline of Jiwani – Balochistan which basically appears due to the change in overall drainage pattern

In contrast to Keti Bunder and Kharo Chann, Jewini area is not much prone to land loss and has comparatively stable shoreline. The results show that erosion and accretion effects are not so prevailing along the jiwani coast. Only change was found on the mouth of Dasht River and its course. Figure 42 illustrates the changing path of DashtRiver from year 1973 to year 2011.

6.5 Meteorological Parameters

Meteorologicalrecords were acquired from Pakistan Meteorological Department of the study area for past thirty years. The graph clearly shows the increasing temperature and decreasing precipitation patterns in the area.

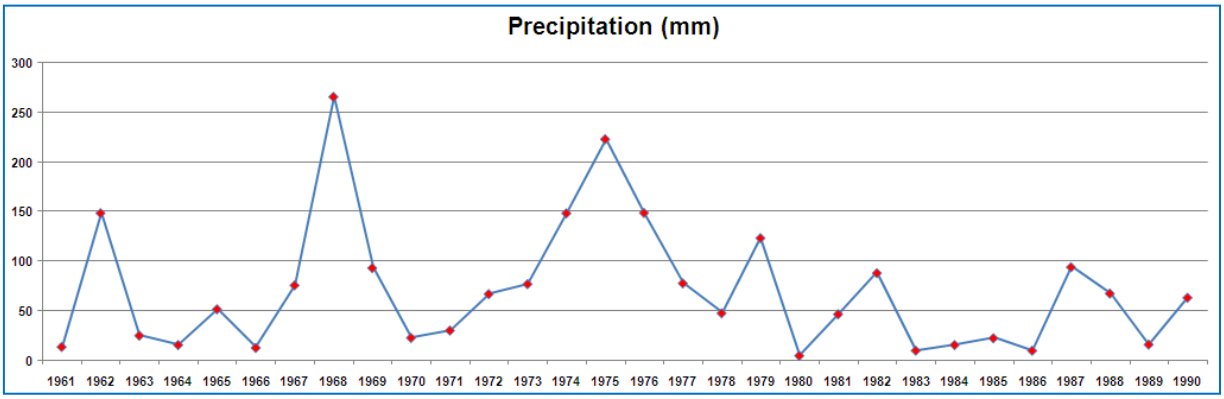

Figure 43: Precipitation Data taken from FY- Meteorological satellite of the Study area in Indus Delta (1961-1990)

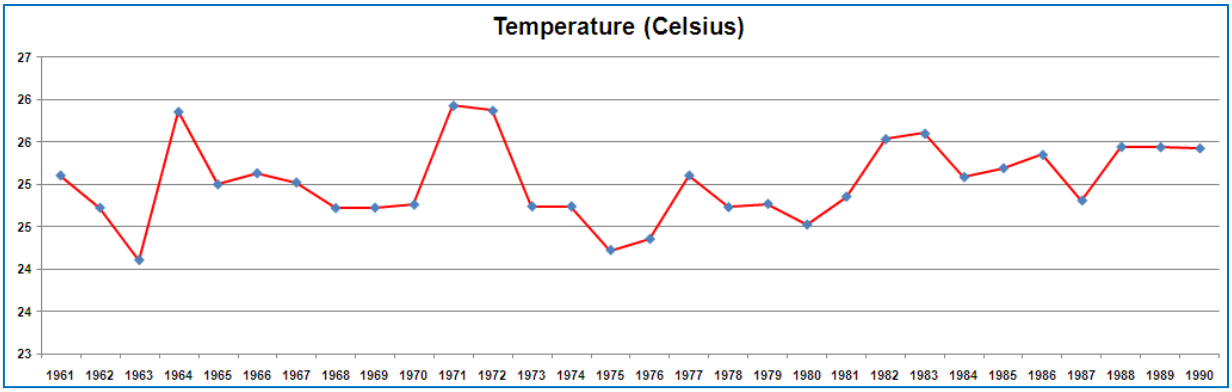

Figure 44: Temperature Data taken from FY- Meteorological satellite of the Study area in Indus Delta (1961-1990)

According to the 4th Assessment Report of the Inter-Governmental Panel on Climate Change (IPCC) released in 2007, a number of GCMs were recommended for downscaling to develop regional climate projections for future. As models were not performing in different regions with the same rate of satisfaction, therefore IPCC engaged scientists from various regions to carry out Model Intercomparison experiments. Among them the fifth experiment is the latest one which is recommended for use in Fifth Climate Assessment Report likely to be released in 2013-14. It has suggested the GCM selection criteria based on following two parameters:

a. Spatial Correlation Coefficient (SCOR) greater than 60%

b. Root-Mean Square Error (RMSE) less than 0.4

A group of GCMs was run for several simulations on the past climate data of Pakistan to reproduce the climatology and the best one was chosen following above criteria. The GCM developed by Max Planks Institute known as ECHAM5 passed the test successfully with good SCOR and the least RMSE.

Selected GCM

ECHAM5 is the 5th generation of the ECHAM general circulation model. Output of ECHAM5 model data for to be used in PRECIS is prepared by the Hadley centre of UK Met office. This data has a horizontal resolution of 140km X 210km. input data is available from 1949 (December) to 2100. The data for the current experiment is obtained from the Hadley Center of UK Met office. All the data sets were converted into GRIBB from NC format which made the accepted format as input to the model.

Data Input

- Mateorological Data of 105 Pakistan station and India, Afghanistan and Iran reported according to WMO format were utilized. Surface and upper air data sets were included along with satellite reanalysis.

- Fine resolution Digital Elevation Model (DEM) was used to realize the terrain features of the selected domain. In total 19 land classifications were used to cater features of climatic zones.

- Observatories data was not on model grids therefore linear and spherical interpolation was carried out with proper nesting and nudging.

• Input was so adjusted that output may take grided spread, visualization by Grads or arranged on excel sheet for any statistical analyses.

Downscaling by Regional Climate Model (RCM) - Brief Description of RCM

PRECIS is a regional climate model developed by Hadley Centre of UK Met Office and it was run on a fast cluster computing system under the Linux operating system. It is a hydrostatic, primitive equation grid point model. There are 19 vertical levels of pressure and 4 levels in the soil (Jones et al., 2004). The model uses the output of different global models GCMs (like HadAM3P, ECHAM4, ECHAM5 etc) and different data sets (like ERA-40, ERA-Interim, etc) for its lateral boundary conditions. The model took one year as spin-up time to allow the land and atmosphere processes to adjust and reach a mutual equilibrium state. Time to complete the experiment depends on the computing capacity of the computer on which the model is run.

The output from the model PRECIS was in post processing (PP) format under the $ARCHIVE/runid/stash-code directory, where runid is the name of the experiment (pmdaa is the runid of current experiment) and stash code is a five digit number used by PRECIS model to represent the different parameters for example the stash code for temperature is 03236. Naming convention of files was required to get the desired daily data files of temperature and precipitation from the output.

Data Extraction (Post processing of the data)

Temperature and precipitation daily data pp files from the output directory are regrided to regular latitude/longitude grid points by using the pp2regrid utility with the PRECIS model software. These regrided pp (post processing) files are then converted to Network Common Data Format (NetCDF) files so that the data can be extracted and displayed through GrADS (Grid Analysis and Display System) software. Grads scripting language is used to get the daily data in CSV (comma separated values) form from these NetCDF files for the period 1950-2099(Dec).

Model Output

Model is run at 0.22° (~=25km) and 0.44° (~=50km) grid resolutions. The number of grid points in are 108X98 and 54X49 respectively for 0.22° (~=25km) and 0.44° (~=50km) grid resolutions. At 0.22° (~=25km) the model has successfully run for the period 1950-2099 with the ECHAM5 data under A1B future scenario. Figure 45 shows the baseline and future scenarios in Thatta district.

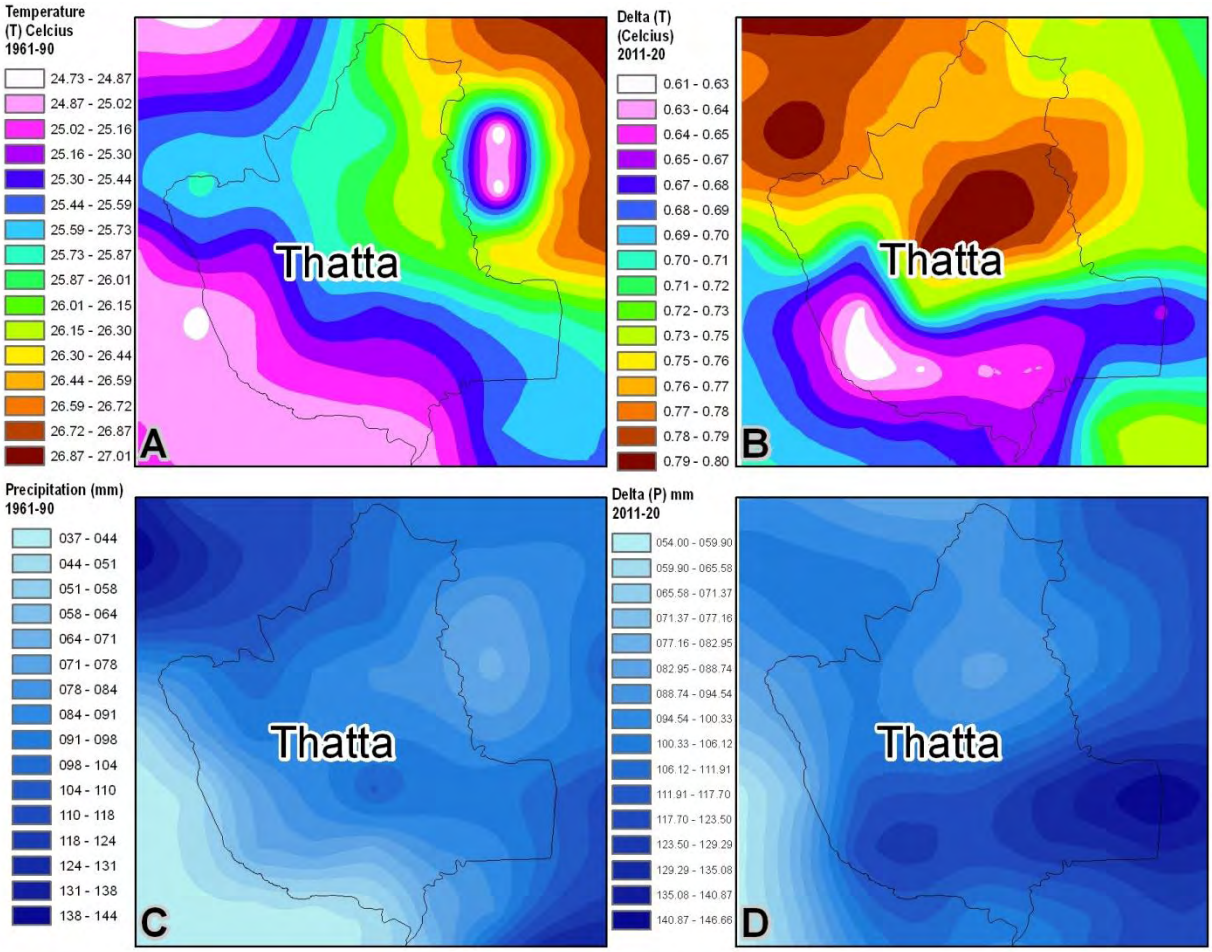

Figure 45: Baseline and predicted values of Temperature and precipitation for Thatta District

6.6 References

Atkinson, P. M., &Massari, R. 1998. Generalized linear modelingof susceptibility to land sliding in the central Apennines, Italy. Computer & Geosciences 24, 373-385

Fielding, A.H. and J.F. Bell. 1997. A review of methods for the assessment of prediction errors in conservation presence/absence models. Environmental Conservation. 24: 38–49.

Knebl, M.R., Yang, Z. L., Hutchison, K., &Maidment, D.R. 2005. Regional Scale Flood Modeling using NEXRAD Rainfall, GIS, and HEC-HMS/RAS: A case study for the San Antonio River Basin Summer 2002 storm event. Journal of Environmental Management, 75, 325–336

Osborne, P.E., J.C. Olonso, R.G. Bryant. 2001. Modelling landscape-scale habitat use using GIS and remote sensing: a case study with Great Bustard. J. Appl. Ecol. 38: 458–471.

Sanyal, J., & Lu, X. X. 2004.Application of remote sensing in flood management with special reference to monsoon Asia – A Review. Natural Hazards 33, Kluwer Academic Publishers.

Zerger, A. 2002.Examining GIS decision utility for natural hazard risk modeling. Environmental Modelling and Software, 17 (3), 287-294